JEM Journal of Experimental Medicine

ARTICLE

Inhibition of hTERT/telomerase/telomere mediates therapeutic efficacy of osimertinib in EGFR mutant lung cancer

Zhen Chen[1], Karin A. Vallega[1], Dongsheng Wang[1], Zihan Quan[2], Songqing Fan[2], Qiming Wang[3], Ticiana Leal[1], Suresh S. Ramalingam[1], and Shi-Yong Sun[1]

The inevitable acquired resistance to osimertinib (AZD9291), an FDA-approved third-generation EGFR tyrosine kinase inhibitor (EGFR-TKI) for the treatment of patients with advanced non-small cell lung cancer (NSCLC) harboring EGFR activating or T790M resistant mutations, limits its long-term clinical benefit. Telomere maintenance via telomerase reactivation is linked to uncontrolled cell growth and is a cancer hallmark and an attractive cancer therapeutic target. Our effort toward understanding the action mechanisms, including resistance mechanisms, of osimertinib has led to the identification of a novel and critical role in maintaining c-Myc–dependent downregulation of hTERT, a catalytic subunit of telomerase, and subsequent inhibition of telomerase/telomere and induction of telomere dysfunction in mediating therapeutic efficacy of osimertinib. Consequently, osimertinib combined with the telomere inhibitor, 6-Thio-dG, which is currently tested in a phase II trial, effectively inhibited the growth of osimertinib-resistant tumors, regressed EGFRm NSCLC patient-derived xenografts, and delayed the emergence of acquired resistance to osimertinib, warranting clinical validation of this strategy to manage osimertinib acquired resistance.

Introduction

The development of various targeted therapies and immunotherapies has substantially impacted the clinical care of lung cancer, a leading cause of cancer death, with an improved 5-year survival rate of up to 20% in the US (Siegel et al., 2022). The milestone discovery of epidermal growth factor receptor (EGFR) activating mutations as a predictor of patient response to EGFR tyrosine kinase inhibitors (EGFR-TKIs) in non-small cell lung cancer (NSCLC) provided a foundation for EGFR-targeted therapy, the first successful targeted therapy against lung cancer, and new insights into the development of other targeted therapies in lung cancer. Although the successes in targeted therapies, including EGFR-targeted therapy, have contributed to improving the quality of life and survival of patients with lung cancer, the inevitable challenge we face in the clinic is the development of acquired resistance that limits their long-term benefits, resulting in eventual treatment failure. To overcome acquired resistance, EGFR-TKIs have evolved rapidly from the early first generation (e.g., erlotinib and gefitinib) and second generation (e.g., afatinib) to the current third generation (e.g., osimertinib or AZD9291) agents. Third-generation EGFR-TKIs are mutation-selective EGFR-TKIs because they selectively and irreversibly bind to and inhibit EGFR mutants harboring activating and T790M resistant mutations with limited activity against wild-type (WT) EGFR. Osimertinib, as the first Food and Drug Administration (FDA)-approved third-generation EGFR-TKI, has been used as a second-line therapy for the treatment of patients with EGFR mutant (EGFRm) NSCLC that has become resistant to first-generation EGFR-TKIs through the T790M mutation and as a first-line option for the therapy of EGFRm advanced NSCLC with very impressive activity in prolonging overall survival of patients (>3 years) (Ramalingam et al., 2020). Unfortunately, acquired resistance inevitably occurs to osimertinib and other third-generation EGFR-TKIs as well (Blaquier et al., 2023; Piper-Vallillo et al., 2020; Zalaquett et al., 2023). Thus, there is an urgent and unmet need in the clinic to develop effective strategies to manage acquired resistance to osimertinib as well as other third-generation EGFR-TKIs.

Acquisition of a novel C797S resistance mutation is a well-defined and the most common EGFR-dependent resistance mechanism to osimertinib particularly when osimertinib is used

[1]Department of Hematology and Medical Oncology, Emory University School of Medicine and Winship Cancer Institute, Atlanta, GA, USA; [2]Department of Pathology, The Second Xiangya Hospital, Central South University, Changsha, China; [3]Department of Internal Medicine, The Affiliated Cancer Hospital of Zhengzhou University, Henan Cancer Hospital, Zhengzhou, China.

Correspondence to Shi-Yong Sun: ssun@emory.edu.

as a second-line therapy. Beyond the EGFR-dependent resistance mechanism, other heterogeneous EGFR-independent mechanisms such as *MET* or *HER2* gene amplification, acquired mutations in oncogenes (e.g., *BRAF*), and small cell or squamous cell transformation have also been reported (Blaquier et al., 2023; Piper-Vallillo et al., 2020; Zalaquett et al., 2023). However, resistance mechanisms in most cases, particularly when osimertinib was used as a first-line therapy, are largely unknown and in active investigation. Preliminary data from the FLAURA trial suggest that resistance to first-line osimertinib may be even more reliant on off-target pathways than resistance to later-line osimertinib (Chmielecki et al., 2023). Thus, fully understanding the mechanisms accounting for the development of acquired resistance to osimertinib or other third-generation EGFR-TKIs will facilitate the development of mechanism-driven strategies for effectively managing the challenging issue of acquired resistance to third-generation EGFR-TKIs, particularly in the first-line setting.

Telomere maintenance via telomerase reactivation has been directly linked to uncontrolled cell growth and thus is a hallmark of cancer cells (Guterres and Villanueva, 2020). In eukaryotic cells, telomerase is a multisubunit ribonucleoprotein complex primarily consisting of a catalytic protein subunit named telomerase reverse transcriptase (TERT) and a central RNA part (TR) or telomerase RNA template (TERC) that is critical for telomeric repeat synthesis (Ghareghomi et al., 2021; Yuan et al., 2019). Human *TERC* is ubiquitously expressed in various human cells while the human *TERT* (*hTERT*) gene is stringently repressed in most human somatic cells, which consequently results in telomerase silencing. Thus, hTERT is a rate-limiting determinant for controlling telomerase activity (Yuan et al., 2019). While telomerase activity is often silenced in most adult somatic or well-differentiated cells, it is reactivated in up to 90% of tumors. Thus, telomerase/telomere represents an attractive and selective cancer target.

hTERT overexpression was associated with poor survival in human solid tumors (Wang et al., 2018). Similarly, *hTERT* expression in NSCLC was also associated with shorter overall survival and disease-free survival (Camps et al., 2006; Hara et al., 2001; Wang et al., 2002, 2018; Zhu et al., 2006) albeit with conflicting results in other studies (Aras et al., 2013; Chen et al., 2017; Metzger et al., 2009; Van den Berg et al., 2010; Wu et al., 2003; Zalewska-Ziob et al., 2017). In preclinical studies, inhibition of human telomerase via dominant negative (DN)-hTERT or small molecules enhanced both chemo- and radiosensitivity of lung cancer cells (Ding et al., 2019; Mender et al., 2018; Misawa et al., 2002). Moreover, EGF was shown to upregulate hTERT via the MEK signaling pathway in NSCLC cells (Lin et al., 2018). EGF was suggested to activate telomerase activity by directly binding to Ets-2 in the *hTERT* promoter in lung cancer cells (Hsu et al., 2015). In A431 and A549 cancer cells with WT EGFR, gefitinib was shown to decrease the expression of *E2F-1* mRNA and protein accompanied by the suppression of *hTERT* mRNA expression and telomerase activity (Suenaga et al., 2006). In another study, it was shown that both erlotinib-sensitive and resistant EGFRm PC-9 cell lines remained sensitive to the telomere inhibitor, 6-thio-2′-deoxyguanosine (6-thio-dG or THIO) (Mender et al., 2018). Although hTERT/telomerase has been connected to chemo- or radioresistance (Lipinska et al., 2017), its impact on the emergence of acquired resistance to targeted therapy, particularly EGFR-targeted therapy, in lung cancer has not been studied.

In our efforts to understand the biology or action mechanisms of osimertinib in sensitive EGFRm NSCLC cells, we found that hTERT expression was downregulated by osimertinib and other EGFR-TKIs in EGFRm NSCLC cells and tissues and exhibited a rebound elevation in osimertinib-resistant cell lines and tumor tissues. Hence, this study focused on demonstrating the role of hTERT/telomerase/telomere suppression in mediating the therapeutic efficacy of osimertinib and the emergence of acquired resistance to osimertinib and on developing a therapeutic strategy via targeting hTERT/telomerase/telomere to manage acquired resistance to osimertinib as well as to other third-generation EGFR-TKIs.

Results

Osimertinib and other EGFR-TKIs downregulate *hTERT* expression in EGFRm NSCLC cells and tumors with inhibition of telomerase and telomere length and induction of telomere dysfunction

To understand the molecular mechanisms by which osimertinib exerts its therapeutic effect in sensitive EGFRm NSCLC cells/tumors, we analyzed RNA sequencing (RNA-seq) data we had previously generated (Zhu et al., 2021) to compare mRNA alterations between DMSO- and osimertinib-treated PC-9 cells and found that the *hTERT* gene was among the top 50 genes altered by osimertinib (Fig. 1 A). This was also true in HCC827 cells (Fig. 1 B). The downregulation of *hTERT* expression was further confirmed by quantitative reverse transcription PCR (RT-qPCR) (Fig. 1 C). Moreover, osimertinib decreased hTERT protein levels in three EGFRm NSCLC cell lines in both concentration- and time-dependent manners (Fig. 1, D and E). Beyond osimertinib, other EGFR-TKIs including erlotinib (first generation), afatinib (second generation), EGF816, CO1686, and HS-10296 (third generation) also decreased hTERT protein levels (Fig. 1 F). As expected, osimertinib did not decrease hTERT levels in NSCLC cell lines with WT EGFR (Fig. 1 G), consistent with its mutation-selective function. Using immunofluorescence (IF), we also detected substantially decreased hTERT levels in EGFRm NSCLC cells (Fig. S1 A) and xenografted tumor tissues (Fig. 1 H) treated with osimertinib in comparison with those in cells or tumors exposed to DMSO or vehicle control. Hence, it is clear that osimertinib and other EGFR-TKIs effectively inhibit *hTERT* expression in EGFRm NSCLC cell lines and tumors.

Given that hTERT is a key activity-determining component of telomerase that controls telomere length, we further determined whether osimertinib inhibits telomerase activity and shortens telomere length in EGFRm NSCLC cells. As expected, we detected significantly reduced telomerase activity and telomere length in both PC-9 and HCC827 cells (Fig. 1, I and J). Hence, osimertinib downregulates hTERT levels accompanied by the suppression of telomerase activity and telomere length. Furthermore, we determined whether osimertinib causes telomere

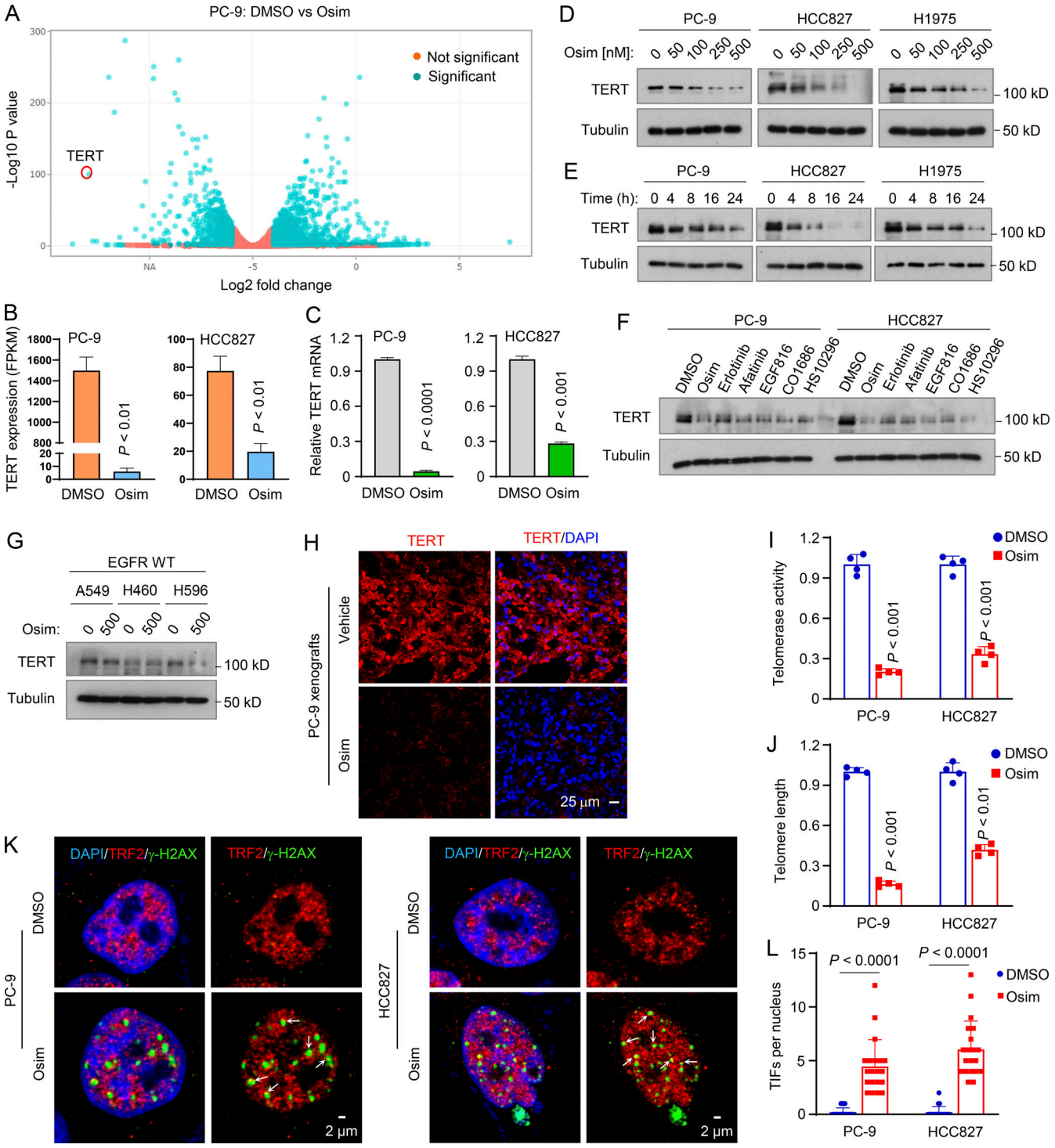

Figure 1. **Osimertinib suppresses hTERT expression accompanied by telomerase/telomere inhibition and TIF induction. (A and B)** RNA-seq data were generated from PC-9 cells treated with DMSO or 100 nM osimertinib (Osim) for 14 h. Each column is the mean ± SD of triplicate treatments. FPKM, fragments per kilobase per million. **(C)** RT-qPCR data for hTERT suppression by osimertinib in the indicated cell lines exposed to DMSO or 100 nM osimertinib for 14 h. Each column is the mean ± SD of triplicate treatments. **(D–G)** The given cell lines were exposed to different concentrations of osimertinib as indicated for 24 h (D), 200 nM osimertinib for varied times as indicated (E), 200 nM indicated EGFR-TKIs for 24 h (F), or 500 nM osimertinib for 24 h (G). The proteins of interest were detected with western blotting. **(H)** IF was used to detect hTERT in PC-9 tumors treated with 15 mg/kg osimertinib for 9 days. **(I and J)** The indicated cell lines were exposed to DMSO or 100 nM osimertinib for 24 h and then subject to telomerase (I) and telomere length (J) assays using the Telomerase Activity Quantification qPCR Assay and Absolute Human Telomere Length Quantification qPCR Assay kits, respectively. The data are means ± SDs of four replicate treatments. **(K and L)** Both PC-9 and HCC827 cell lines were treated with 200 nM osimertinib for 24 h followed with the TIF assay. TIFs were counted from 20 cells for each treatment and represented as means ± SEs. Arrows indicate TIFs (colocalization of TRF2 and γ-H2AX). Statistical differences were assessed with two-sided unpaired Student's *t* test. Source data are available for this figure: SourceData F1.

dysfunction or stress by conducting a telomere dysfunction-induced foci (TIF) assay to detect the colocalization of γ-H2AX, a DNA damage marker, and TRF2, a protein present in telomeres, by IF staining. This assay allowed us to identify and distinguish telomere-specific damage signals from non-telomeric genomic DNA damage. As presented in Fig. 1, K and L, osimertinib significantly increased TIFs in addition to inducing an overall increase in genomic DNA damage in both PC-9 and HCC827 cell lines. Hence, it is clear that osimertinib induces telomere-specific DNA damage and telomere dysfunction.

Osimertinib downregulates *hTERT* expression via suppressing c-Myc–dependent transactivation of *hTERT* gene in EGFRm NSCLC cells

To understand the mechanism(s) by which osimertinib inhibits *hTERT* expression, we searched putative transcriptional factors that may bind to the *hTERT* promoter region and regulate *hTERT* transcription (Fig. 2 A) and also assessed modulation of the expression of these transcriptional factor genes by osimertinib generated in our RNA-seq analyses (Fig. 2 B). As a result, c-Myc gained our attention among these transcriptional factors because it was the most downregulated by osimertinib in both PC-9 and HCC827 cell lines (Fig. 2 B) and is known to regulate *hTERT* transcription through two E-boxes (or c-Myc binding sites) in the *hTERT* core promoter region (Dratwa et al., 2020; Yuan et al., 2019). Moreover, our published data showed that osimertinib and other EGFR-TKIs effectively decreased the levels of c-Myc in EGFRm NSCLC cell lines and tumors primarily through an ERK inhibition–dependent induction of protein degradation (Zhu et al., 2021). Indeed, we found that c-Myc reduction occurred ahead of hTERT decrease in cells exposed to osimertinib (Fig. 2 C), and both c-Myc and hTERT reduction co-occurred in these cell lines as detected with IF (Fig. 2 D and Fig. S1 B). c-Myc knockdown using both siRNA and shRNA in the tested EGFRm NSCLC cell lines accordingly caused a reduction of hTERT levels (Fig. 2, E and F). Conversely, enforced overexpression of ectopic *c-Myc* and particularly degradation-resistant mutant *c-Myc* (S62A) genes rescued hTERT reduction induced by osimertinib (Fig. 2 G). Enforced overexpression of ectopic *c-Myc* (T58A) exerted a similar effect as c-Myc did (Fig. S1 C). These data suggest a tight connection between c-Myc reduction and hTERT downregulation in EGFRm NSCLC cells induced by osimertinib. Analysis of the Cancer Genome Atlas program (TCGA) database also showed a significant and positive correlation between *c-Myc* and *hTERT* expression in EGFRm NSCLCs (Fig. S2 A). Either high *c-Myc* or *hTERT* expression in EGFRm NSCLCs was significantly associated with worse survival of patients (Fig. S2, B and C). These findings further support the tight connection between *c-Myc* and *hTERT* expression in EGFRm NSCLC.

We further determined the effect of osimertinib on hTERT gene promoter activity and its dependence on c-Myc using the core promoter regions of *hTERT* gene with and without E-boxes or c-Myc binding sites, one upstream located at around −186 and another downstream located at +22 (Veldman et al., 2001, 2003) (Fig. 2 H). As presented in Fig. 2 I, osimertinib significantly inhibited the luciferase activity of hTERT-luc reporter constructs with both E-boxes (−255/+5) or one E-box (−88/+40), but not the construct (−130/+5) without these E-boxes, in both PC-9 and HCC827 cell lines. Hence, it is clear that osimertinib inhibits *hTERT* transcription in a c-Myc–dependent manner.

hTERT expression is inversely associated with survival in patient with NSCLC and is elevated in osimertinib-resistant cell lines with resistance to osimertinib modulation and in EGFRm NSCLC tissues relapsed from EGFR-TKI treatment

Previous studies of the prognostic value of hTERT expression in human NSCLC generated inconsistent results although some demonstrated that high hTERT expression is significantly associated with poor prognosis (Aras et al., 2013; Camps et al., 2006; Chen et al., 2017; Hara et al., 2001; Metzger et al., 2009; Van den Berg et al., 2010; Wang et al., 2018; Wang et al., 2002; Wu et al., 2003; Zalewska-Ziob et al., 2017; Zhu et al., 2006). We therefore detected hTERT expression in human NSCLCs including lung squamous cell carcinoma and adenocarcinoma using immunohistochemistry (IHC) (Fig. S2 D) and found that hTERT expression was significantly elevated in these NSCLC tissues compared with that in normal tissues (Fig. S2 E) and tumors positive for hTERT expression were significantly associated with poor patient survival (Fig. S2, F and G). Since increased hTERT/telomerase has been connected to drug resistance such as chemoresistance (Lipinska et al., 2017), we then analyzed our RNA-seq data and found that *hTERT* expression was significantly elevated in PC-9/AR cells (PC-9 cells with acquired resistance to osimertinib) compared with that in PC-9 parental cells (Fig. 3 A). This finding was confirmed with RT-qPCR in both PC-9/AR and HCC827/AR cells (Fig. 3 B). Moreover, several osimertinib-resistant NSCLC cell lines possessed higher levels of baseline hTERT than their corresponding parental cell lines and were resistant to osimertinib modulation in terms of hTERT reduction, as evaluated with western blotting (Fig. 3 C). Similar results were generated in EGFRm NSCLC cell lines with acquired resistance to HS-10296 (HSR; Fig. 3 D). Elevated basal levels of hTERT were also observed in three additional EGFRm NSCLC cell lines with acquired resistance to osimertinib (Fig. 3 E). By IF staining, osimertinib treatment clearly reduced hTERT staining signals in PC-9 cells, but not in PC-9/AR cells, which showed stronger staining signals than those in PC-9 cells (Fig. 3 F). Similar results were also generated in HCC827 and HCC827/AR cells (Fig. 3 F).

Moreover, we compared telomerase activity and telomere length between parental cell lines and their corresponding osimertinib-resistant cell lines. As presented in Fig. 3, G and H, both telomerase activities and telomere lengths in PC-9/AR and HCC827/AR cell lines were significantly higher than those in their corresponding parental cell lines, indicating that osimertinib-resistant EGFRm NSCLC cells possess elevated telomerase activity and telomere length.

In samples of EGFRm NSCLC tissues relapsed from first-generation EGFR-TKIs including erlotinib, gefitinib, or icotinib, hTERT elevation was detected in 66.7% (12/18) of resistant cases in comparison with their corresponding pretreatment baseline tissues (Fig. 3, I and J). Similar results were generated in tissues relapsed from osimertinib (62.5%, 5/8; Fig. 3, I and J). In

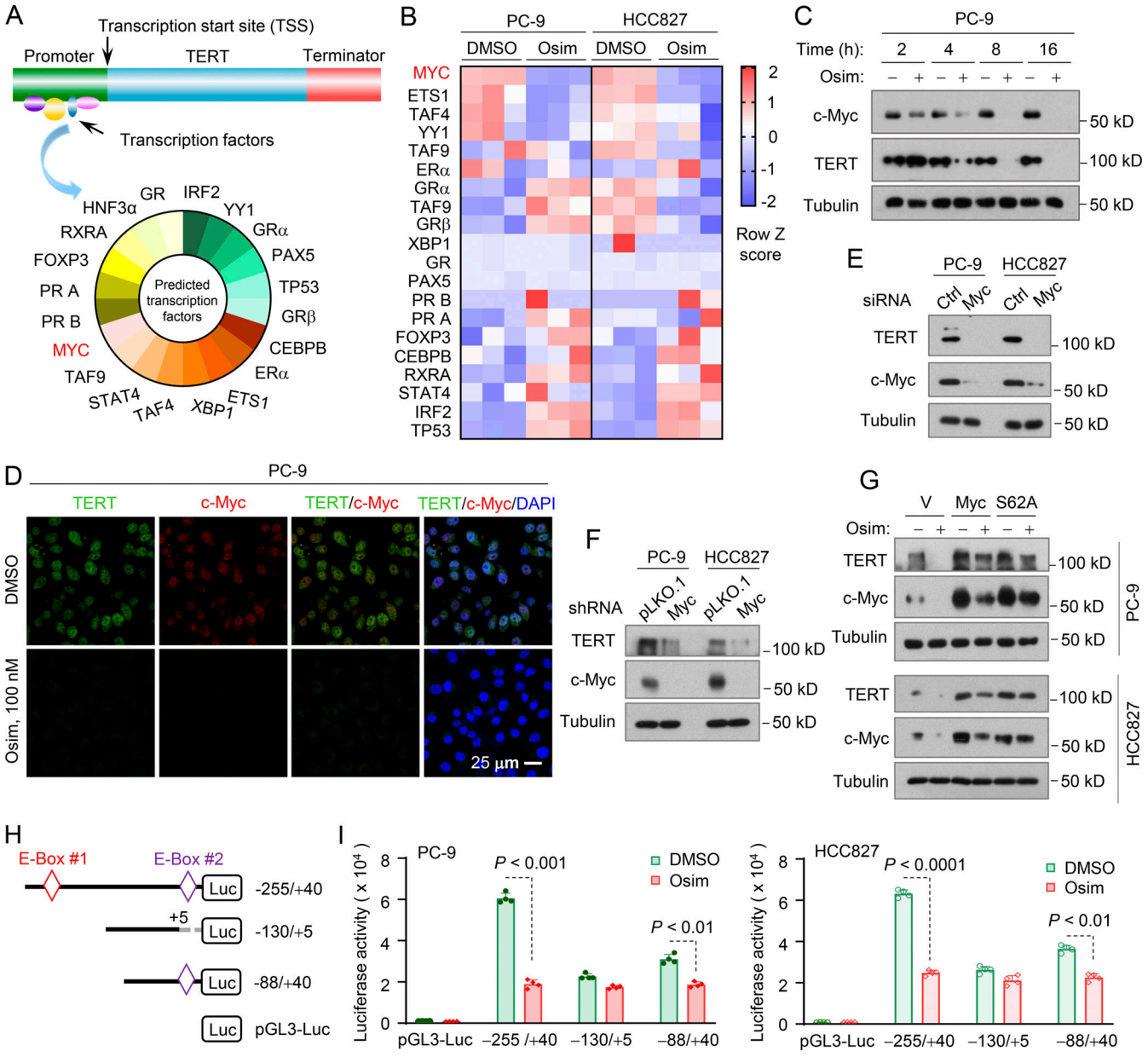

Figure 2. **c-Myc suppression mediates downregulation of *hTERT* expression by osimertinib. (A)** Putative transcriptional factors were predicted with PROMO program. **(B)** Alterations of transcriptional factors in RNA-seq data generated from both PC-9 and HCC827 cells treated with DMSO or 100 nM osimertinib (Osim) for 14 h presented in the heatmap (triplicate treatments). **(C and D)** PC-9 cells were exposed to 200 nM for the indicated times (C) or 24 h (D), **(E)** The indicated cell lines were transfected with the indicated siRNAs for 48 h. **(F)** The indicated cell lines were infected with lentiviruses carrying hTERT shRNA followed by puromycin selection. **(G)** The indicated cell lines expressing ectopic vector (V), WT, and mutant *c-Myc* genes, respectively, were exposed to DMSO or 200 nM osimertinib (Osim) for 16 h. After the aforementioned treatments, the proteins of interest were detected with western blotting (C and E–G) or IF (D). **(H)** Reporter constructs harboring the core *hTERT* promoter region and deleted regions. **(I)** The indicated cell lines were transfected with the given reporter constructs for 24 h followed by 200 nM osimertinib for another 16 h. Cells were then harvested for luciferase assay. The data are the means ± SD of four replicate determinations. Statistical differences were assessed with two-sided unpaired Student's *t* test. Source data are available for this figure: SourceData F2.

general, hTERT levels in the relapsed tissues were significantly elevated in comparison with the baseline levels before treatment. Therefore, hTERT expression is clearly increased in the majority of EGFRm NSCLC tissue relapsed from EGFR-TKIs. These data collectively suggest that hTERT elevation is tightly associated with the emergence of acquired resistance to osimertinib as well other EGFR-TKIs.

hTERT modulation regulates response of EGFRm NSCLC cells to osimertinib in decreasing cell survival and inducing apoptosis

We anticipated that suppression of *hTERT* expression, e.g., with gene knockdown, in osimertinib-resistant cells may restore their sensitivity to osimertinib if elevated hTERT plays a critical role in conferring resistance to osimertinib. Indeed, knockdown

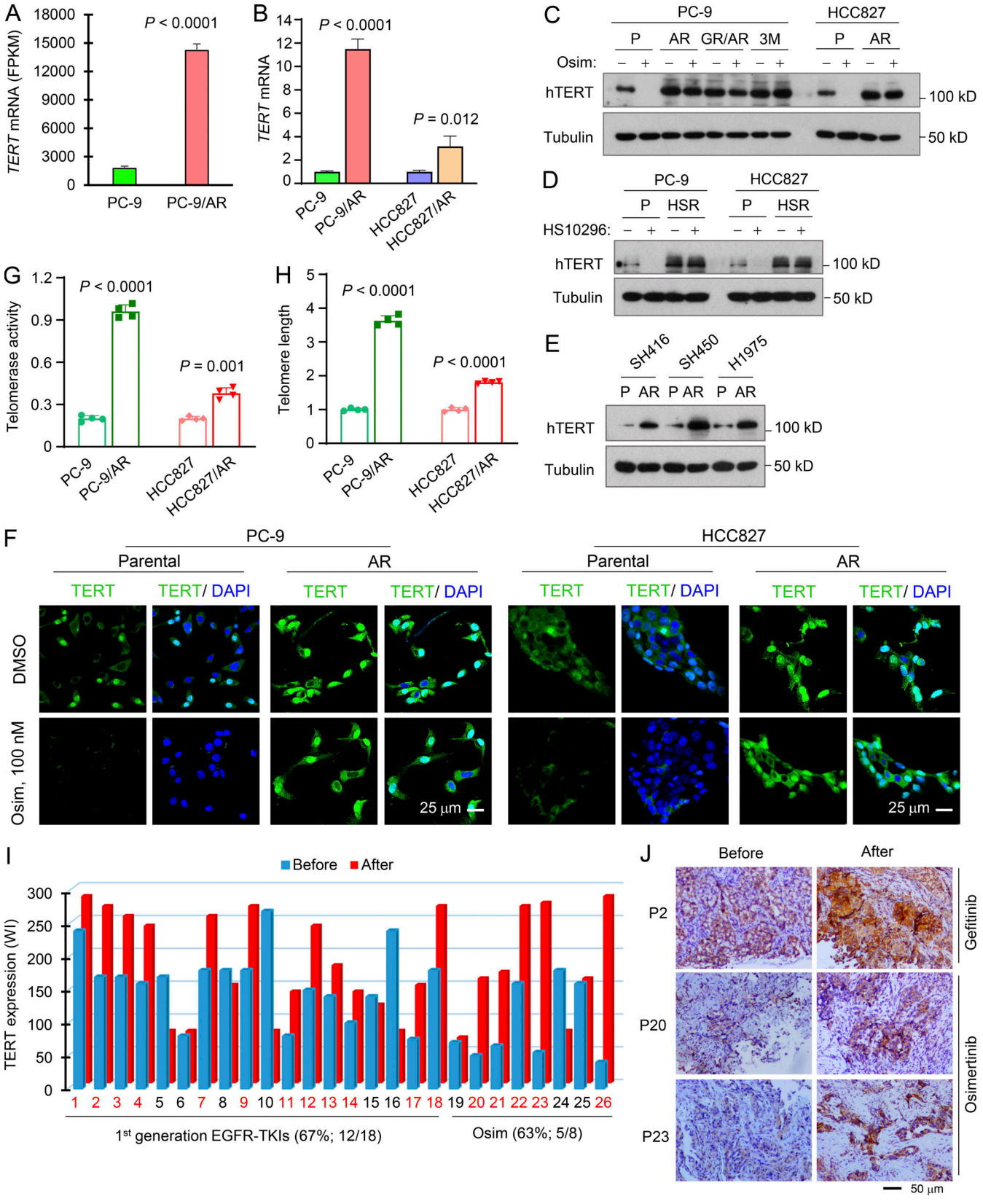

Figure 3. ***hTERT* expression is elevated in EGFRm NSCLC cell lines and patient tumor tissues with acquired resistance to osimertinib. (A)** RNA-seq data for hTERT upregulation in osimertinib-resistant PC-9 cells. Each column is the mean ± SD of triplicate treatments. **(B)** RT-qPCR detection of *hTERT* mRNA levels in the indicated cell lines. Each column is the mean ± SD of triplicate treatments. **(C–E)** Western blotting detection of hTERT protein from the indicated cell lines with or without exposure to 200 nM osimertinib (Osim) or HS-10296 for 16 h (C and D) or basal levels of TERT in the indicated cell lines (E). P, parental; AR, AZD9291-resistant; HSR, HS-10296-resistant. **(F)** IF detection of hTERT in the indicated cell lines exposed to 100 nM osimertinib for 24 h. **(G and H)**

Telomerase activity (G) and telomere length (H) in the tested cell lines were detected using the Telomerase Activity Quantification qPCR Assay and Absolute Human Telomere Length Quantification qPCR Assay kits, respectively. The data are the means ± SDs of four replicate determinations. **(I and J)** hTERT in human EGFRm NSCLC issues were detected with IHC and representative pictures of hTERT staining are shown (J). WI, weight index, which represents % positive stain × intensity score (0–3). Statistical differences were assessed with a two-sided unpaired Student's *t* test. Source data are available for this figure: SourceData F3.

of *hTERT* expression with either *hTERT* siRNA or shRNA in different osimertinib-resistant EGFRm NSCLC cell lines enhanced the ability of osimertinib to induce the cleavage of both caspase-3 and PARP and to increase annexin V-positive cells and to decrease cell numbers (Fig. 4, A–F), indicating restoration of the sensitivity of the osimertinib-resistant cell lines to osimertinib. In contrast, enforced overexpression of ectopic *hTERT* in the osimertinib-sensitive cell lines, PC-9 and HCC827, substantially compromised the effects of osimertinib on inducing PARP cleavage, increasing annexin-V positive cells, and reducing cell numbers (Fig. 4, G–I), thus conferring resistance to osimertinib. Collectively, it is apparent that modulation of *hTERT* expression impacts the responses of EGFRm NSCLC cell lines to osimertinib, suggesting a critical role of hTERT suppression in mediating the therapeutic efficacy of osimertinib.

Osimertinib in combination with a telomerase or telomere inhibitor exerts augmented effects on decreasing cell survival and inducing Bim-dependent apoptosis in osimertinib-resistant cell lines together with the enhanced induction of TIFs

To potentially translate our findings to a realistic strategy in the clinic for the treatment of EGFRm NSCLC relapsed from EGFR-TKI treatment, we then screened several small molecules with telomerase- or telomere-inhibitory activity for their abilities to synergize with osimertinib in suppressing the growth of osimertinib-resistant cells. 6-Thio-dG is a nucleoside analog and telomerase substrate that is incorporated into de novo–synthesized telomeres, leading to telomere dysfunction and rapid cell death in telomerase-positive cancer cells (Guterres and Villanueva, 2020; Mender et al., 2015). MST-312 is a telomerase inhibitor that can effectively reduce telomere length in cancer cells (Seimiya et al., 2002). RHPS4 is a G-quadruplex–stabilizing telomerase inhibitor that displaces hTERT from the nucleus, leading to the induction of telomere-initiated DNA-damage signaling as well as chromosome fusions (Cookson et al., 2005; Gowan et al., 2001). These different telomerase or telomere inhibitors, when combined with osimertinib, could synergistically decrease the survival of both HCC827/AR and PC-9/AR cell lines (combination indexes [CIs] < 1; Fig. 5 A and Fig. S3). Hence, it is clear that inhibition of telomerase or telomere with different inhibitors restores, at least partially, the response of osimertinib-resistant cell lines to osimertinib.

6-Thio-dG, the only telomere-by-telomerase targeting agent currently in development, is now being tested in a Phase 2 clinical study in NSCLC in combination with the checkpoint inhibitor, cemiplimab (NCT05208944). Therefore, we chose to primarily focus on 6-Thio-dG in our following experiments. Beyond the augmented effects on decreasing survival, the combination of osimertinib and 6-Thio-dG was significantly more effective than each agent alone in suppressing colony formation and growth of both PC-9/AR and HCC827/AR cell lines (Fig. 5 B) in the long-term colony formation assay that allows us to repeat the treatments for a relatively long period of time. Consistently, the combination was much more potent than either single agent in inducing cleavage of caspase-3 and PARP (Fig. 5 C) and increasing annexin V-positive cell populations (Fig. 5 D) in different osimertinib-resistant cell lines, indicating augmentation of apoptosis in these osimertinib-resistant cell lines.

Osimertinib is known to modulate Mcl-1 and Bim levels, resulting in Bim-dependent apoptosis (Shi et al., 2017). Hence, we further determined the effects of the osimertinib and 6-Thio-dG combination on modulating the levels of Mcl-1 and Bim in different osimertinib-resistant cell lines. As shown in Fig. 5 E, the combination of osimertinib and 6-Thio-dG clearly and robustly elevated Bim levels accompanied with a reduction of Mcl-1 levels, whereas either single agent had little or no effect. Moreover, the combination lost its augmented effects on the induction of apoptosis, evidenced by the failure to enhance PARP cleavage and increase annexin V-positive cells, in both PC-9/AR-Bim/KO and HCC827/AR-Bim/KO cell lines, in which Bim was knocked out (Fig. 5, F and G). Taken together, the combination of osimertinib and 6-Thio-dG clearly enhances Bim-dependent apoptosis in osimertinib-resistant EGFRm NSCLC cells.

6-Thio-dG is known to induce telomere dysfunction (Mender et al., 2015, 2020). We thus further determined whether the combination of osimertinib with 6-Thio-dG enhances the suppression of telomere function in osimertinib-resistant cells. By performing the TIF assay, we observed that the combination of osimertinib and 6-Thio-dG was significantly more active than either agent alone in increasing TIFs in both PC-9/AR and HCC827/AR cells, which were insensitive to TIF induction by osimertinib (Fig. 5, H and I), indicating the enhanced effect of the combination on induction of telomere dysfunction in osimertinib-resistant cells.

The combination of osimertinib and 6-Thio-dG effectively inhibits the growth of osimertinib-resistant tumors in nude mice with enhanced induction of apoptosis

Following the above in vitro promising results, we then evaluated the effects of the osimertinib and 6-Thio-dG combination on the growth of different osimertinib-resistant xenografted tumors in nude mice. While osimertinib (5 mg/kg/day) and 6-Thio-dG alone had minimal growth-inhibitory effects, their combination effectively and significantly retarded the growth of both PC-9/AR and HCC827/AR tumors by measuring both tumor size and tumor weight (Fig. 6, A–C). Moreover, the body weights of mice receiving the combination were not significantly

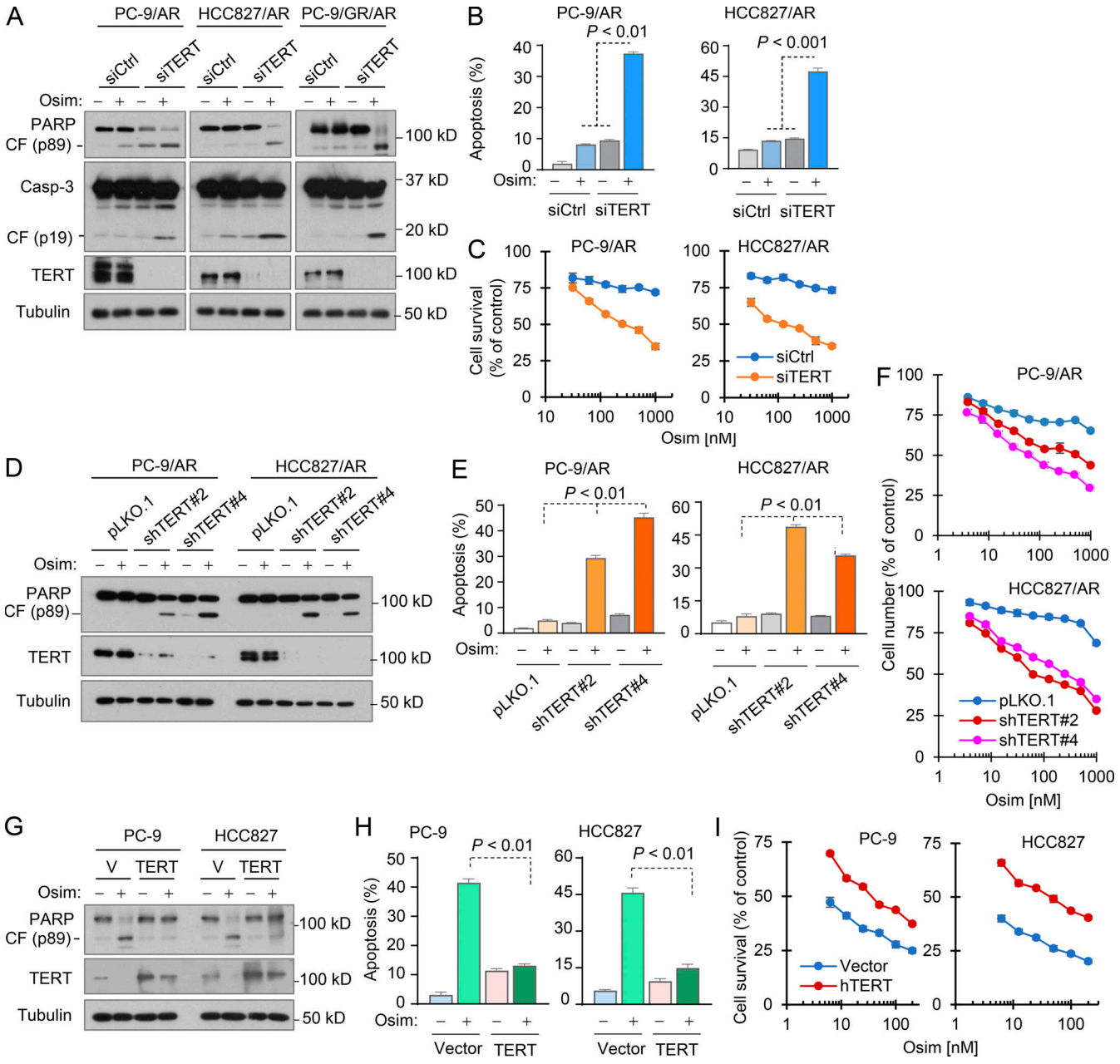

Figure 4. **Genetic manipulations of *hTERT* expression alter the responses of EGFRm NSCLC cell lines to osimertinib. (A–F)** The indicated cell lines transfected with scrambled control or *hTERT* siRNA for 48 h (A–C) or expressing pLKO.1 or shTERT (D and E) were exposed to DMSO or 200 nM osimertinib (Osim) for 24 h (A and D), 48 h (B and E), or 72 h (C and F). **(G–I)** The indicated cell lines expressing vector (V) or *hTERT* gene were exposed to DMSO or 100 nM osimertinib for 24 h (G), 48 h (H), or 72 h (I). The proteins of interest were detected with western blotting (A, D, and G). Annexin V-positive cells were determined with flow cytometry (B, E, and H). Cell numbers were estimated with the SRB assay (C, F, and I). The data are means ± SDs of triplicate (B, E, and H) or four replicate (C, F, and I) determinations. Statistical analysis was conducted with one-way ANOVA test (B) or two-sided unpaired Student's *t* test (E and H). CF, cleaved form. Source data are available for this figure: SourceData F4.

different from those in other groups of mice (Fig. S4, A and B). Moreover, we did a similar experiment with bigger initial tumor sizes (over 200 mm^3) and a high dosage of osimertinib at 15 mg/kg/day, which is equivalent to 80 mg daily in patients, and generated similar outcomes (Fig. S4, C–E). Hence, it is apparent that the combination of osimertinib and 6-Thio-dG is very effective in inhibiting the growth of osimertinib-resistant tumors with favorable tolerability in vivo. In agreement, we detected many more cells positive for cleaved PARP (cPARP) and Bim levels and fewer cells positive for Ki-67 and Mcl-1 in tumors treated with the combination of osimertinib and 6-Thio-dG in comparison with those exposed to either treatment agent alone (Fig. 6 D). Consistently, the combination effectively suppressed the phosphorylation of EGFR and ERK, whereas each agent alone minimally or did not do so (Fig. S4 F). These results together indicate that the combination enhances suppression of EGFR signaling with augmented induction of apoptosis in addition to suppression of cell proliferation.

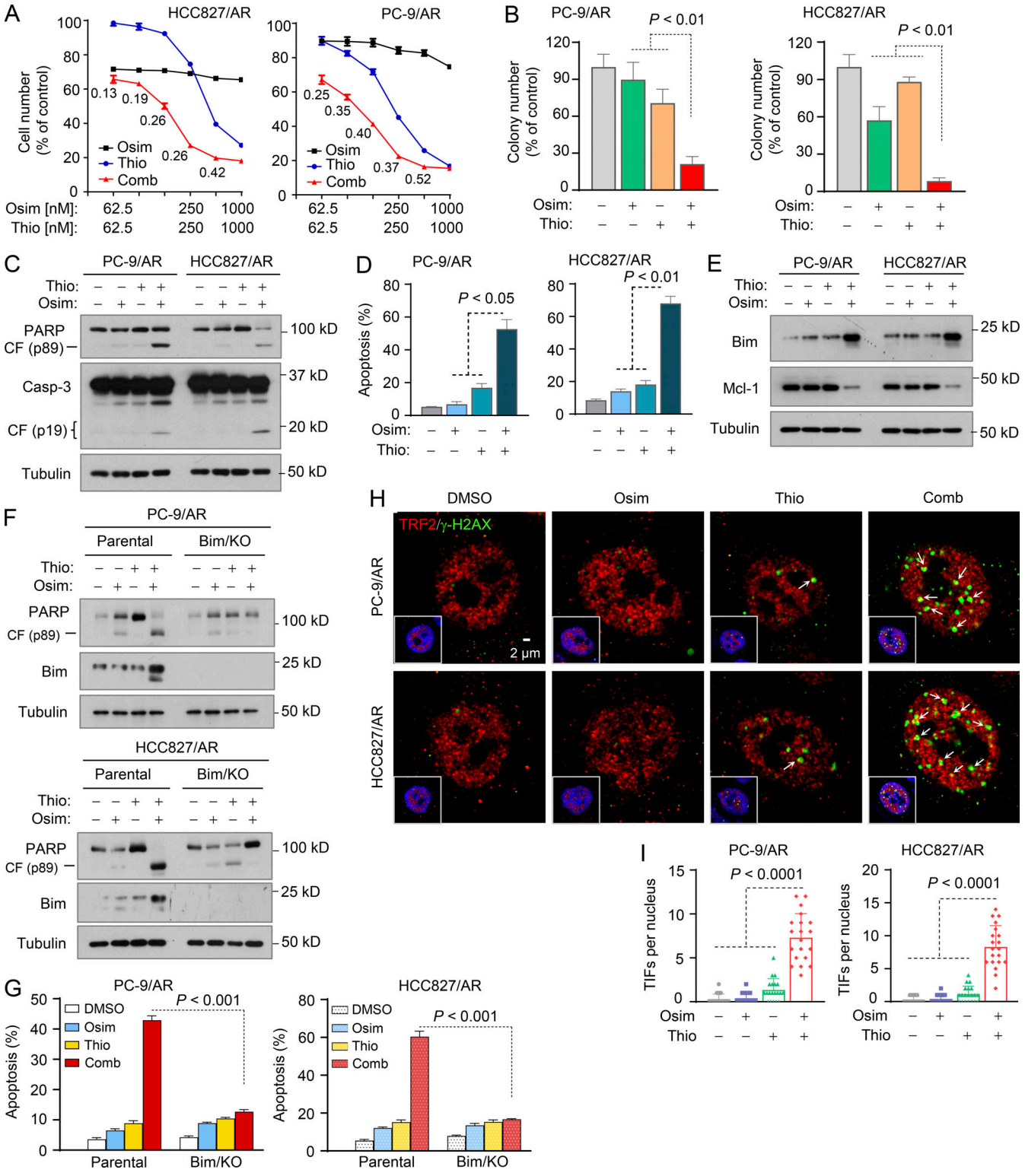

Figure 5. **6-Thio-dG in combination with osimertinib synergistically induces apoptosis and TIFs in osimertinib-resistant EGFRm NSCLC cell lines. (A)** The given cell lines were treated with varied concentrations of the tested agents either alone or in combinations for 3 days. Cell numbers were then measured by SRB assay and CIs were calculated and presented inside the graph. The data are means ± SDs of four replicate determinations. **(B)** The tested cell lines seeded in 12-well plates were treated with 50 nM osimertinib, 50 nM 6-Thio-dG (Thio), or their combination, which were repeated with fresh medium every 3 days. After 10 days, the cells were fixed, stained with crystal violet dye, imaged, and counted. Columns are means ± SDs of triplicate determinations. **(C–G)** The tested cell lines were exposed to 200 nM osimertinib, 250 nM 6-Thio-dG or their combination for 16 h (E), 24 h (C and F), or 48 h (D and G). The proteins of interest were detected with western blotting (E, C, and F) and apoptotic cells were detected with annexin V staining/flow cytometry (D and G). Each column represents mean ± SD of triplicate treatments. **(H and I)** Both PC-9/AR and HCC827/AR cells were treated with 200 nM osimertinib, 250 nM 6-Thio-dG, or their combination for 24 h followed by the TIF assay. TIFs were counted from 20 cells for each treatment and represented as means ± SEs. The inserted images show

costaining of DAPI, TRF2 and γ-H2AX. Arrows indicate TIFs (colocalization of TRF2 and γ-H2AX). Statistical analysis was conducted with one-way ANOVA test (B, D, and I) or two-sided unpaired Student's *t* test (G). Source data are available for this figure: SourceData F5.

The combination of osimertinib and 6-Thio-dG augments therapeutic efficacy against the growth of EGFRm NSCLC patient-derived xenografts (PDXs) induces tumor regression and delays the emergence of acquired resistance to osimertinib

In addition to the above experiments focusing on cell lines and tumors with acquired resistance to osimertinib, we also determined the effects of osimertinib and 6-Thio-dG combination on the survival of a few PC-9–derived cell lines with primary resistance to osimertinib (Gu et al., 2020) possessing elevated levels of hTERT (Fig. 7 A). The combination was more effective than either agent alone in decreasing the survival of the three cell lines with primary resistance to osimertinib with CIs of <1 (Fig. 7, B and C), indicating synergistic effects. Moreover, the combination was effective in eliminating drug-tolerant cells (DTCs) of both PC-9 and HCC827 cells since DTCs were detected in the cell lines exposed to osimertinib but not in the cell lines treated with the combination of osimertinib and 6-Thio-dG (Fig. 7 D). Given that the presence of primarily resistant clones and DTCs in sensitive EGFRm NSCLC cell populations represents a key mechanism accounting for the emergence of acquired resistance to EGFR-TKIs (Cabanos and Hata, 2021; Sun, 2023), we next determined the effects of the combination on suppressing the growth of EGFRm NSCLC tumors and delaying the emergence of acquired resistance to osimertinib. The three EGFRm NSCLC PDXs, TM00193, TM00219, and particularly TM00199, were all responsive to osimertinib treatment (at a dosage of 5 mg/kg/day, which effectively suppressed EGFR signaling evidenced by decreasing p-EGFR and p-ERK levels in both PC-9 and HCC827 xenografts; Fig. S5 A) albeit with varied degrees of sensitivity. Among them, TM00193 was relatively less sensitive to osimertinib. It did not respond well to osimertinib in the initial period of the treatment but responded after 20 days although the growth was only retarded (Fig. 7 E and Fig. S5 B). TM00219 and particularly TM00190 were relatively sensitive to osimertinib but did grow back as treatment times were prolonged (Fig. 7, F and G; and Fig. S5, C and D), indicating the appearance of acquired resistance. All three PDXs were initially sensitive to 6-thio-dG in the initial period of the treatment (e.g., up to 40 days) under the tested conditions and then gradually became less responsive to treatment (Fig. 7, E–G and Fig. S5), suggesting the emergence of resistance. Although the osimertinib and 6-Thio-dG combination in each model did not clearly enhance the inhibition of tumor growth in the early phase of the treatment in comparison with osimertinib alone, it did shrink tumors or induce tumor regression from about day 40 until the end of the treatment, which was over 100 days, while tumors receiving osimertinib or 6-Thio-dG alone continued to gradually grow larger (Fig. 7, E–G and Fig. S5). In the TM00199 model, the tumor suppressive effect of the combination was maintained upto over 180 days (Fig. 7 G and Fig. S5 D). These results solidly demonstrate that the addition of 6-Thio-dG to EGFR-targeted therapy, e.g., with osimertinib, leads to an augmented therapeutic efficacy and delays or even prevents the emergence of acquired resistance. Under the tested conditions with the different EGFRm NSCLC PDXs, mice treated with the combination had body weights comparable to those treated with osimertinib alone even after a prolonged period of over a 100-day treatment (Fig. S5, E–G), demonstrating the favorable tolerability of the combination while augmenting therapeutic efficacies against the growth of EGFRm NSCLC tumors.

Discussion

hTERT/telomerase has been connected to chemo- and radioresistance (Lipinska et al., 2017). However, it is unknown whether modulation of hTERT/telomerase plays a role in regulating cell response of EGFRm NSCLC to EGFR-targeted therapy, particularly with osimertinib and other third-generation EGFR-TKIs. It was shown previously that both erlotinib-sensitive and resistant EGFRm PC-9 cell lines remained sensitive to 6-thio-dG monotherapy (Mender et al., 2018), but whether inhibition of telomere or telomerase has a role in overcoming the emergence of acquired resistance to EGFR-TKIs has remained unstudied. In this study, we found that the expression of hTERT, a key component of the telomerase enzyme complex, and telomerase activity including telomere length were significantly inhibited with induction of telomere dysfunction by osimertinib as well other EGFR-TKIs in sensitive EGFRm NSCLC cell lines. Once the cells became resistant to osimertinib or other third-generation EGFR-TKIs, hTERT basal levels were elevated and could not be reduced further by osimertinib in these resistant cell lines. Correspondingly, telomerase activity and telomere length were significantly increased in osimertinib-resistant cell lines. We confirmed hTERT elevation in the majority of EGFRm NSCLC tissues relapsed from EGFR-TKIs including osimertinib. Accordingly, knockdown of *hTERT* in these resistant cell lines restored cell sensitivity to osimertinib in terms of cell number reduction and apoptosis induction, whereas enforced overexpression of ectopic *hTERT* in sensitive EGFRm NSCLC cell lines conferred resistance to osimertinib. Hence, we have identified a novel and critical role of hTERT/telomerase or telomere inhibition in mediating the therapeutic efficacy of osimertinib, establishing a previously undiscovered connection between the modulation of hTERT/telomerase or telomere and cell responses of EGFRm NSCLC to osimertinib, and likely other third-generation EGFR-TKIs. In addition to these findings, we further showed that some telomerase or telomere inhibitors, particularly 6-Thio-dG, like hTERT gene knockdown, synergistically decreased the survival of osimertinib-resistant EGFRm NSCLC cells with augmented induction of telomere dysfunction and apoptosis and effectively inhibited the growth of osimertinib-resistant tumors in vivo. These data thus provide compelling evidence in support of targeting hTERT/telomerase/telomere as an effective strategy for overcoming acquired resistance to osimertinib and other third-generation EGFR-TKIs.

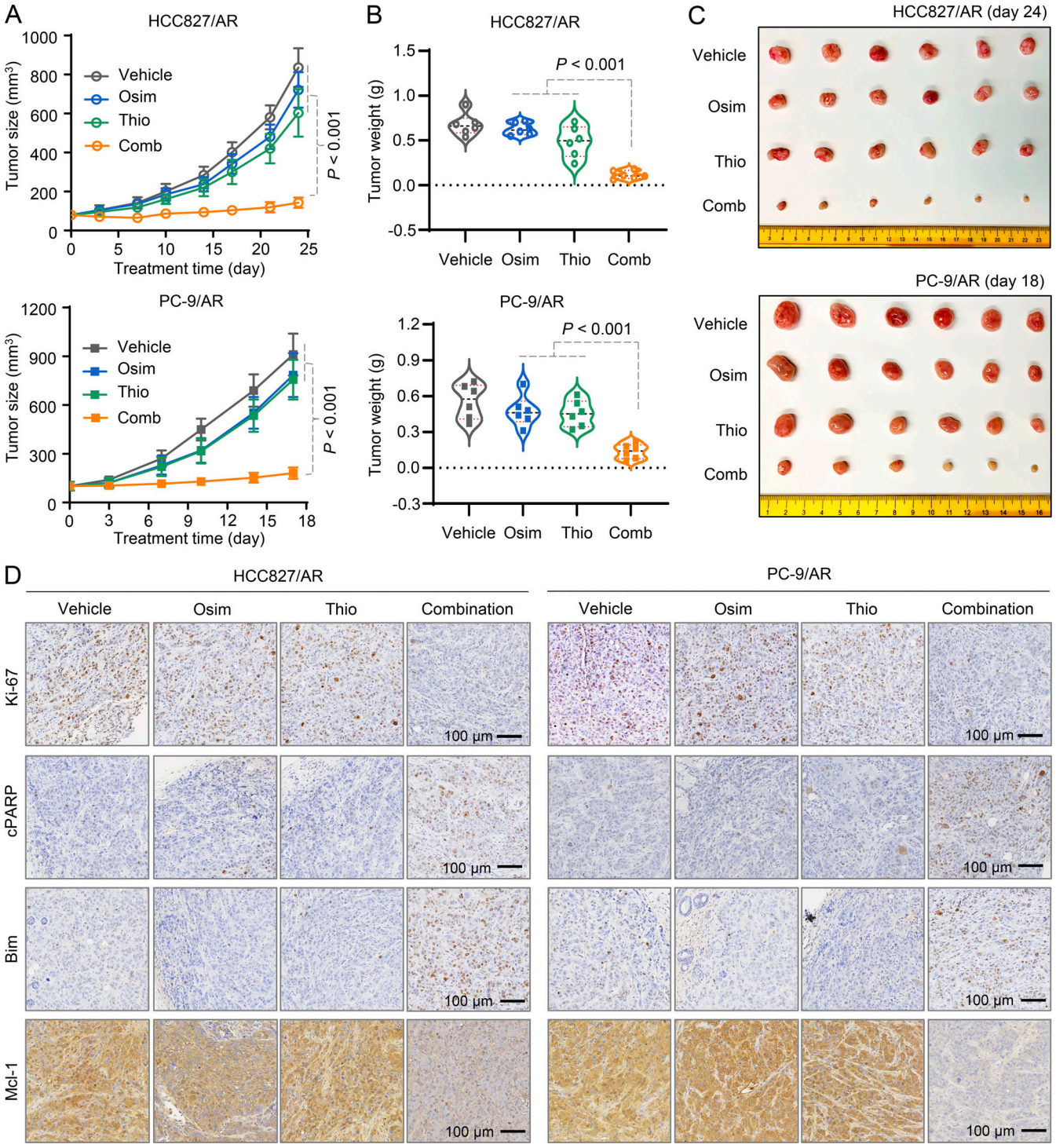

Figure 6. **The combination of osimertinib with 6-Thio-dG effectively inhibits the growth of osimertinib-resistant EGFRm NSCLC xenografts.** HCC27/AR or PC-9/AR cells grown in NU/NU nude mice as xenografted tumors (n = 6/group) were treated with vehicle, osimertinib alone (5 mg/kg, daily, oral gavage [og]), 6-Thio-dG (Thio) alone (2.5 mg/kg/day, daily, intraperitoneal injection [ip]), or their combination. (A) Tumor sizes were measured at the indicated time points (A). **(B and C)** At the end of treatment, tumors in each group were also weighed (B) and photographed (C). The data in each group are means ± SEs of six tumors from six mice. **(D)** The proteins of interest as indicated were stained with IHC (D). Statistical analysis was conducted with one-way ANOVA test.

It is known that telomere shortening can result in telomere dysfunction, resulting in a DNA damage response that leads to apoptosis (Deng et al., 2008). Our previous study has shown that osimertinib induces DNA damage via inhibition of TOPO II in EGFRm NSCLC cells (Chen et al., 2024). The current study clearly shows that osimertinib significantly induced telomere dysfunction-induced DNA damage as assessed by the detection of increased TIFs in these cell lines as well, suggesting

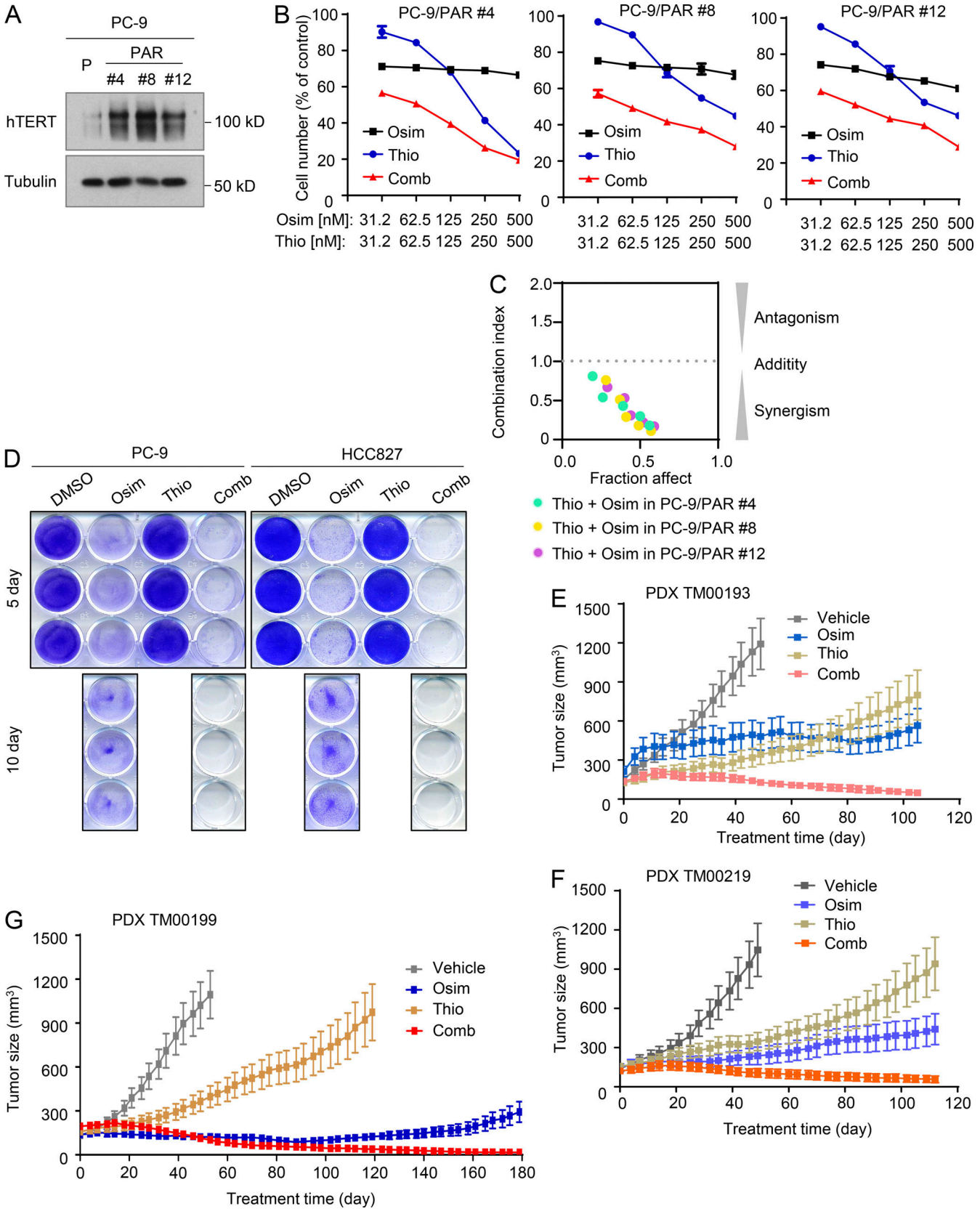

Figure 7. **Osimertinib and 6-Thio-dG combination eliminates DTCs and regresses different EGFRm PDX tumors with long-term remissions. (A)** Detection of baseline hTERT expression in the indicated EGFRm NSCLC cell lines with primary osimertinib resistance by western blotting. **(B and C)** The given cell lines were exposed to varied concentrations of osimertinib (Osim), 6-Thio-dG (Thio) alone, or their combination. After 3 days, cell numbers were determined with the SRB assay (B). The data are means ± SDs of four replicate determinations. CIs for the combinations were also calculated (C). **(D)** The indicated cell lines

seeded in 12-well plates were treated with 50 nM osimertinib, 50 nM 6-Thio-dG, or their combination; these treatments were repeated with fresh medium every 2 days. After 5 or 10 days, the cells were fixed, stained with crystal violet dye, and pictured. **(E–G)** The indicated PDXs in nude mice (six tumors/group) were treated with vehicle, 5 mg/kg osimertinib (daily, og), 2.5 mg/kg 6-Thio-dG (daily, ip), or their combination. The data are means ± SEs of six tumors. Source data are available for this figure: SourceData F7.

another mechanism by which osimertinib induces DNA damage although telomeric DNA represents only about 1/6,000th of the total genomic DNA (Mender et al., 2015). This finding together with our previous observation reinforced the critical role of DNA damage induction in mediating apoptosis and therapeutic efficacy of osimertinib against EGFRm NSCLC.

Taking early preventive interventions using effective and tolerable combination regimens that interfere with the process of developing acquired resistance offers an active approach and may substantially improve the long-term survival benefit of EGFRm NSCLC treatment with osimertinib (Sun, 2023). Beyond the effect on overcoming acquired resistance to osimertinib, our study has also demonstrated that the inclusion of 6-Thio-dG early in osimertinib treatment of EGFRm NSCLC tumors before resistance occurs effectively caused tumor regression without seeing relapse after a long period of treatment (>100 days), whereas tumors receiving osimertinib treatment alone resumed growth, indicating a potential of the combination strategy in delaying or even preventing emergence of acquired resistance to osimertinib or other third-generation EGFR-TKIs. Furthermore, we did not see enhanced toxicity in mice treated with the combination for even up to 180 days, indicating that the combination treatment is well tolerated in mice. Based on current knowledge, the presence of primarily resistant clones and DTCs in the EGFRm NSCLC cell population constitutes a key mechanism accounting for the emergence of acquired resistance to EGFR-TKIs including osimertinib (Cabanos and Hata, 2021; Sun, 2023). Hence, the promising effect of this combination on inducing tumor regression and delaying or preventing the emergence of acquired resistance is likely due to its effectiveness in eliminating both primarily resistant clones and DTCs as demonstrated in this study.

Although few studied telomerase or telomere inhibitors have progressed to the clinic, 6-Thio-dG, as a first-in-class small molecule that is the only telomere-by-telomerase targeting agent currently in development, has now advanced to a Phase 2 clinical study in NSCLC as the first study to test 6-Thio-dG's immune system activation followed by administration of the checkpoint inhibitor cemiplimab (NCT05208944). Moreover, FDA has recently granted orphan drug designation to 6-Thio-dG for the treatment of small-cell lung cancer in addition to hepatocellular carcinoma (https://www.onclive.com/view/fda-grants-orphan-drug-designation-to-thio-in-small-cell-lung-cancer). The promising preclinical efficacy of 6-Thio-dG combined with osimertinib as demonstrated in this study warrant the clinical evaluation of the combination for its potential in overcoming acquired resistance to osimertinib or other third-generation EGFR-TKIs and in delaying or preventing the emergence of acquired resistance to prolong the survival of EGFRm NSCLC patients.

In this study, hTERT elevation was detected in over 65% of EGFRm NSCLC tissues from patients whose disease relapsed from treatment with EGFR-TKIs including osimertinib. Hence, the combination strategy of osimertinib with 6-Thio-dG is a promising strategy in these relapsed NSCLC with elevated hTERT. Therefore, the detection of hTERT elevation may be used as a predictive biomarker for selecting patients with disease relapse from osimertinib treatment to receive this therapeutic strategy to achieve possible clinical benefit. The current finding on hTERT elevation in EGFRm NSCLCs relapsed from EGFR-TKI treatment were all generated in Chinese patients. Hence, further studies are needed to verify this finding in EGFRm NSCLC tumors arising in other ancestries receiving EGFR-TKI treatment.

The outcomes of studying the impact of hTERT expression in NSCLC on patient survival have remained inconsistent. While some studies showed that high hTERT expression was associated with shorter overall survival and disease-free survival (Camps et al., 2006; Hara et al., 2001; Wang et al., 2002, 2018; Zhu et al., 2006), others demonstrated no survival impact of hTERT expression or even the opposite results (Aras et al., 2013; Chen et al., 2017; Metzger et al., 2009; Van den Berg et al., 2010; Wu et al., 2003; Zalewska-Ziob et al., 2017). This is likely due to the small sample sizes of some studies and the different detection assays used (IHC and RT-qPCR). In our study, we used IHC to detect NSCLC tissues positive for hTERT in a sample size of 196 NSCLC cases and found that hTERT positivity was significantly associated with poor survival. Hence, the expression of hTERT does have a critical impact on the survival of NSCLC patients.

c-Myc is a critical transcriptional factor that positively regulates *hTERT* expression (Dratwa et al., 2020; Yuan et al., 2019). In our previous study, we showed that osimertinib as well as other EGFR-TKIs effectively decreased the levels of c-Myc in EGFRm NSCLC cell lines and tumors primarily through facilitating protein degradation in addition to transcriptional suppression (Zhu et al., 2021). Moreover, targeting c-Myc with either genetic knockdown or indirect chemical inhibition restored the responses of osimertinib-resistant cells and tumors to osimertinib (Zhu et al., 2021). In the current study, we demonstrated that osimertinib downregulated the expression of *hTERT* in a c-Myc–dependent manner and targeting hTERT or telomerase/telomere in osimertinib-resistant cells and tumors generated similar outcomes as targeting c-Myc. Hence, it is likely that inhibition of the c-Myc/hTERT axis constitutes a critical mechanism accounting for the therapeutic efficacy of osimertinib and likely other third-generation EGFR-TKIs against EGFRm NSCLC. In addition to c-Myc, it was reported that EGF increases hTERT expression through Ets-2-mediated hTERT promoter transactivation in lung cancer cells (Hsu et al., 2015). The current study does not rule out the possible role of Ets-2 in mediating the suppression of *hTERT* expression by osimenrtinib. Based on our RNA-seq data, osimertinib did not inhibit *ETS2*

gene expression in both PC-9 and HCC827 cell lines (data not shown). Thus, the likelihood of Ets-2 in mediating suppression of hTERT expression by osimenrtinib is low.

In summary, the current study has identified a previously undiscovered novel connection between modulation of hTERT/telomerase/telomere and the response of EGFRm NSCLC cells/tumors to osimertinib and likely other third-generation EGFR-TKIs, thus providing a new therapeutic strategy to overcome and delay or prevent acquired resistance to osimertinib as well as other third-generation EGFR-TKIs via targeting hTERT, telomerase, or telomere. The compelling preclinical findings presented in this study also warrant clinical validation of targeting telomerase or telomeres to manage osimertinib-acquired resistance.

Materials and methods

Reagents and expression constructs

6-Thio-dG, MST-312, and RHPS4 were purchased from MedChemExpress (MCE). hTERT antibody (#DF7129) for western blotting and IF staining was purchased from Affinity Biosciences. hTERT (sc-377511) for IHC and Mcl-1 (sc-12756) antibodies were purchased from Santa Cruz Biotechnology. Bim (#2933), c-Myc (#5605), and cleaved PARP (cPARP; #5625) antibodies were purchased from Cell Signaling Technology, Inc. TRF2 antibody (EPR3517[2]) (ab108997) was purchased from Abcam. Ki-67 rabbit monoclonal antibody (MA5-14520), DAPI (#62248), secondary antibodies Alexa Fluor 488-Donkey anti-mouse (A32766), and Alexa Fluor 568-Donkey anti-rabbit (A10042) were purchased from Thermo Fisher Scientific. Other reagents and antibodies were the same as described previously (Chen et al., 2021; Shi et al., 2017). *c-Myc* and *c-Myc* (S62A) expression constructs, which were described previously (Zhu et al., 2021), together with *c-Myc* (T58A) expression construct in the same vector was provided Dr. Junran Zhang (The Ohio State University, Columbus, OH, USA). pLV-hTERT-IRES-hygro (#85140; Addgene) (Hayer et al., 2016) and matched vector pLV-EF1a-IRES-Hygro (#85134; Addgene) were purchased from Addgene.

Cell lines and cell culture

All cell lines used in this study were described previously (Chen et al., 2022; Gu et al., 2020; Zhu et al., 2021). PC-9/AR/Bim-KO and HCC827/AR/Bim-KO cell lines were established using the same method as described in our previous study (Chen et al., 2022). The cell lines that stably overexpress the ectopic *hTERT* gene were established with infection of lentiviruses carrying an *hTERT* gene followed by hygromycin selection. These cell lines were not genetically authenticated. All cell lines were cultured in RPIM1640 medium supplemented with 5% FBS at 37°C in 5% CO_2 humidified air.

Colony formation assay

Tested cell lines were seeded in 12-well plates at a density of 150 or 200 cells/well. After 24 h, the cells were exposed to the tested drugs. The medium was replaced with a fresh medium containing the same drugs every 3 days. After 10 days, the medium was removed and the cell colonies were fixed, stained with 2% crystal violet in ethanol, and counted.

Cell survival assay

Cells seeded in 96-well plates at appropriate densities one day before the treatment were exposed to tested drugs either alone or in combination for 3 days. Cell numbers were measured by sulforhodamine B (SRB) assay as previously described (Sun et al., 1997). CI for drug interaction was calculated with the CompuSyn software (ComboSyn, Inc.).

Apoptosis assays

Apoptosis was evaluated with the annexin V/7-AAD apoptosis detection kit (BD Biosciences) following the manufacturer's protocol. Apoptosis was also demonstrated by the detection of protein cleavages with western blotting.

Western blot analysis

The procedures used for the preparation of whole-cell protein lysates and immunoblotting were described previously (Shi et al., 2017). Protein band intensities were quantified by NIH ImageJ software.

RT-qPCR

Cellular total RNA was extracted using an RNA extraction kit (Qiagen) according to the manufacturer's instructions. The concentrations were measured with NanoDrop (Thermo Fisher Scientific) and reverse transcription was carried out using the RevertAid First Strand cDNA Synthesis Kit (Qiagen). qPCRs were performed at 95°C for 15 s followed by 40 cycles of 95°C for 5 s and 60°C for 30 s using the QuantStudio 3 and 5 systems (Thermo Fisher Scientific). The primer pairs for hTERT were 5′-GCCGATTGTGAACATGGACTACG-3′ (forward) and 5′-GCTCGTAGTTGAGCACGCTGAA-3′ (reverse). GAPDH was used as an endogenous control and detected with the primers of 5′-GTCTCCTCTGACTTCAACAGCG-3′ (forward) and 5′-ACCACCCTGTTGCTGTAGCCAA-3′. All primers were synthesized from Integrated DNA Technologies.

Telomerase activity assay

Telomerase activity assay was conducted using Telomerase Activity Quantification qPCR Assay Kit (Cat #8928; ScienCell Research Laboratories) according to the manufacturer's instructions. In brief, cells exposed to DMSO or osimertinib for 24 h were resuspended in lysis buffer and incubated at 4°C for 30 min. After centrifugation at 12,000 *g* for 20 min at 4°C, the supernatant was incubated with telomerase reaction buffer at 37°C for 3 h for telomerase reaction. Samples were heated at 85°C for 10 min to stop the reaction followed by qPCR with telomere primer set.

Telomere length assay

Cells exposed to given treatments were harvested for extraction of DNA with the QIAamp DNA Investigator Kit (Cat#56504) according to the manufacturer's protocol. Telomere length was then determined by qPCR with the Absolute Human Telomere Length Quantification qPCR Assay Kit (Cat#8918; ScienCell

Research Laboratories) following the manufacturer's instructions. In brief, each PCR reaction contained a genomic DNA sample (0.01 µg/µl), telomere primer, 2× qPCR master mix, and nuclease-free water. Reference genomic DNA was used as an internal control. Amplification was performed under the following conditions: denaturation for 10 min at 95°C followed by 32 cycles of denaturation for 20 s at 95°C, annealing for 20 s at 52°C, and extension for 45 s at 72°C. The average telomere lengths were calculated following the manufacturer's instructions.

TIF assay

The TIF assay was conducted as described previously (Mender et al., 2015) by detecting the colocalization of DNA damage with γ-H2AX antibody that recognizes broken double-stranded DNA and telomeres using the telomeric shelterin protein, TRF2, antibody. In brief, cells seeded on chamber slides and exposed to a given treatment for a certain time were washed with PBS three times. Slides were fixed with 4% paraformaldehyde (PFA) for 10 min and then incubated with blocking solution (0.2% fish gelatin and 0.5% BSA) for 30 min at room temperature. After incubation, slides were incubated with primary antibodies (anti-γ-H2AX 1:100 or anti-TRF2 1:100) diluted in a blocking solution overnight at 4°C. After washing with PBS three times, slides were incubated with secondary antibodies (Alexa Fluor 488-Donkey anti-mouse 1:200 or Alexa Fluor 568-Donkey anti-rabbit 1:200) for 1 h at room temperature. Slides were viewed before mounting in a medium containing DAPI. Images were collected using the confocal microscope (TCS SP8; Leica).

Prediction of transcription factor binding sites

Putative transcription factor binding sites were predicted with PROMO program (Farré et al., 2003; Messeguer et al., 2002) (https://alggen.lsi.upc.es/cgi-bin/promo_v3/promo/promoinit.cgi?dirDB=TF_8.3).

Transient transfection and luciferase reporter assay

The given cells plated in 24-well plates were transfected with an hTERT reporter plasmid together with pCH110 plasmid harboring β-galactosidase gene using Fugene 6 reagent (Roche Applied Science) following the manufacturer's protocol. After 24 h, the cells were treated with DMSO or osimertinib for another 16 h and then harvested in cell-lysis buffer for measurement of luciferase activity with the Luciferase Assay kit (Promega) using a Sirius Luminometer (Berthold Detection Systems). Luciferase activity was normalized with β-galactosidase activity, which was measured as described previously (Pfahl et al., 1990). All hTERT reporter constructs described previously (Veldman et al., 2001, 2003) were kindly provided by Dr. Xuefeng Liu (Ohio State University; Columbus, OH, USA).

Gene knockdown using siRNA and shRNA

hTERT siRNA (sc-36641), *hTERT* shRNA plasmid (sc-36641-SH), *c-Myc* siRNA (sc-29226), and *c-Myc* shRNA plasmid (sc-29226-SH) were purchased from Santa Cruz Biotechnology. Scrambled control siRNA and the procedures used for transfection were described previously (Chen et al., 2021).

DTCs

Cells seeded in 12-well plates at a density of close to 90% were exposed to the tested drugs. The cells were refed with fresh medium containing the same drugs every 2 days. After 5 or 10 days, the medium was removed to fix and stain DTCs with 2% crystal violet in ethanol.

TCGA data analysis

The Kaplan–Meier analysis was performed using EGFR TKI–treated patient data retrieved from TCGA LUAD datasets (http://cancergenome.nih.gov/). Patients were stratified according to high versus low expression (cutoff: median) of *hTERT* or *c-Myc* within their tumors.

Human NSCLC tissues

Paired tissue samples from patients with EGFRm NSCLC before treatment (i.e., baseline) and after disease relapse from the treatment with an EGFR-TKI including gefitinib or osimertinib were collected at the Second Xiangya Hospital (Changsha, Hunan, China) and Henan Cancer Hospital (Zhengzhou, Henan, China) under Ethics Review Committee (IRB)-approved protocols (Xiangya IRB2019-009, Henan IRB2019-067 and Emory IRB00104138). All tissues were sent to and stained at the Second Xiangya Hospital. Tissue arrays with 196 cases of NSCLC tissue samples from patients who underwent surgical treatment in the Department of Thoracic Surgery under the approved IRB protocol (IRB2021-K021) were generated in the Department of Pathology at the Second Xiangya Hospital.

IF

Tissue slides or cells grown on chamber slides were fixed with 4% PFA for 10 min, washed with PBS three times, and then incubated with 5% BSA containing 0.2% Triton X-100 for 30 min. After incubation, slides were exposed to primary antibodies (anti-hTERT 1:100 or anti-c-Myc 1:100) overnight at 4°C followed by incubation with a second antibody Alexa Fluor 488-Donkey anti-mouse (1:200) or Alexa Fluor 568-Donkey anti-rabbit (1:200) for another 1 h at room temperature. Slides were mounted in a medium containing DAPI. Images were collected using the confocal microscope (Leica TCS SP8).

IHC

IHC staining of xenografted tissues was done basically as described previously (Chen et al., 2021) using different primary antibodies at given dilutions, respectively (hTERT 1:100, Ki-67 1:100, cPARP 1:50, Bim 1:200 and Mcl-1 1:100). Human NSCLC tissues were stained using the EnVision + Dual Link System-HRP Kit (Dako) as described previously (Zhang et al., 2021). hTERT antibody (#DF7129; Affinity Biosciences) was diluted at 1:1,000. The staining data was finally quantified as a weight index (WI) that represents % positive stain in the tumor multiplied by intensity score (0–3) as described previously (Elrod et al., 2010).

Animal xenograft and treatments

Animal experiments were approved by the Institutional Animal Care and Use Committee (IACUC) of Emory University. In the conventional cell-derived xenograft studies, cells suspended in

sterile PBS at 3×10^6 per mouse were injected into the flank of 4-wk-old nu/nu nude mice purchased from The Jackson Laboratory. On day 7, when the average tumor volumes were 100 or 200 mm^3, the mice were divided into groups with equal average tumor volumes and body weights. The following treatments were administered daily: vehicle, osimertinib (5 or 15 mg/kg, og), 6-Thio-dG (2.5 mg/kg, ip), and the combination of osimertinib and 6-Thio-dG. Tumor volume was measured using calipers every 2 or 3 days and calculated by $V = \pi$ (length × width^2)/6. Body weight was also measured every 2 or 3 days. At the end of the experiment, mice were sacrificed using CO_2. The tumors were then removed, weighed, and stored in formalin for further analysis.

In PDX studies, the three PDXs harboring different EGFR mutations, TM00193 (E746_A750del), TM00199 (L858R), and TM00219 (E746_A750del; T790M; exon 19 del), were purchased from The Jackson Laboratory. When the average tumor volumes were around 100 mm^3, the mice received the same treatments as described above. Tumor volume was measured using calipers every 3 or 4 days.

For the above animal experiments, vehicle and osimertinib treatment groups were shared with other treatments as described in our previous study (Chen et al., 2024) to minimize the utilization of mice.

Statistical analysis

Two-sided unpaired or paired Student's *t* test was used to determine statistical differences between the two groups. One-way ANOVA test was conducted to value differences among multiple groups. Results are presented as means ± SDs or SEs. All statistical analyses were conducted using Graphpad Prism 9.0 software. P values <0.05 were considered statistically significant.

Online supplemental material

Fig. S1 shows that osimertinib reduces hTERT or both c-Myc and hTERT levels in EGFRm NSCLC cells as evaluated with IF and modulates hTERT levels in EGFRm NSCLC cell lines expressing ectopic *c-Myc* or *c-Myc* T58A mutant gene. Fig. S2 shows hTERT expression in human NSCLC tissues, its association with c-Myc expression, and its impact on patient survival. Fig. S3 shows that osimertinib in combination with other telomerase inhibitors synergistically decreases the survival of osimertinib-resistant cell lines. Fig. S4 shows that the combination of osimertinib with 6-Thio-dG is well tolerated in nude mice with enhanced effects on inhibiting the growth of osimertinib-resistant PC-9/AR tumors and on suppressing EGFR/ERK signaling in vivo. Fig. S5 shows that osimertinib at a dosage that effectively suppresses EGFR signaling combined with 6-Thio-dG potentiates NSCLC tumor regression and delays tumor relapse with good tolerability in mice.

Data availability

All data acquired specifically for this study, including raw western blotting data, are available within the article itself and its supplementary materials.

Acknowledgments

We are grateful to Dr. Anthea Hammond in our department for editing the manuscript, to Dr. Junran Zhang (The Ohio State University, Columbus, OH, USA) for providing *c-Myc* expression constructs, and Dr. Xuefeng Liu (The Ohio State University, Columbus, OH, USA) for providing *hTERT* reporter constructs. We are also thankful to Zhenxing Guo who is currently in the School of Data Science, The Chinese University of Hong Kong-Shenzhen (Shenzhen, Guangdong, China) for helping with TCGA data analysis. S.S. Ramalingam and S.-Y. Sun are Georgia Research Alliance Distinguished Cancer Research Scholars.

This work was supported by National Institutes of Health/National Cancer Institute grants UG1 CA233259 (to S.S. Ramalingam and T. Leal), R01 CA223220 (S.-Y. Sun), R01 CA245386 (S.-Y. Sun), and R01 CA284386 (S.-Y. Sun).

Author contributions: Z. Chen: Conceptualization, Data curation, Formal analysis, Investigation, Methodology, Visualization, Writing—original draft, K.A. Vallega: Investigation, Resources, Writing—review & editing, D. Wang: Investigation, Z. Quan: Data curation, Formal analysis, Investigation, S. Fan: Resources, Q. Wang: Data curation, Investigation, Resources, Writing—review & editing, T. Leal: Conceptualization, Visualization, Writing—original draft, Writing—review & editing, S.S. Ramalingam: Conceptualization, Supervision, Writing—original draft, Writing—review & editing, S.-Y. Sun: Conceptualization, Formal analysis, Funding acquisition, Project administration, Supervision, Writing—original draft, Writing—review & editing.

Disclosures: T. Leal reported personal fees from AstraZeneca, Daiichi-Sankio, Janssen, Takeda, EMD Serono, Eisai, Novocure, Amgen, Roche/Genentech, Regeneron, Jazz, Catalyst, OncoC4, Pfizer, Novartis, Bristol Myers Squibb, AbbVie, Gilead, Black Diamond, and Boehringer-Ingelheim outside the submitted work. S.S. Ramalingam reported grants from Bristol Myers Squibb, AstraZeneca, Merck, Pfizer, and Amgen outside the submitted work. No other disclosures were reported.

Submitted: 8 March 2024
Revised: 7 July 2024
Accepted: 26 August 2024

References

Aras, G., D. Kanmaz, N. Urer, S. Purisa, F. Kadakal, E. Yentürk, and E. Tuncay. 2013. Immunohistochemical expression of telomerase in patients with non-small cell lung cancer: Prediction of metastasis and prognostic significance. *Anticancer Res.* 33:2643–2650.

Blaquier, J.B., S. Ortiz-Cuaran, B. Ricciuti, L. Mezquita, A.F. Cardona, and G. Recondo. 2023. Tackling osimertinib resistance in EGFR mutant non-small cell lung cancer. *Clin. Cancer Res.* 29:3579–3591. https://doi.org/10.1158/1078-0432.CCR-22-1912

Cabanos, H.F., and A.N. Hata. 2021. Emerging insights into targeted therapy-tolerant persister cells in cancer. *Cancers.* 13:2666. https://doi.org/10.3390/cancers13112666

Camps, C., R. Sirera, R.M. Bremnes, V. Ródenas, A. Blasco, M.J. Safont, J. Garde, A. Juarez, C. Caballero, J.J. Sanchez, et al. 2006. Quantification in the serum of the catalytic fraction of reverse telomerase: A useful prognostic factor in advanced non-small cell lung cancer. *Anticancer Res.* 26:4905–4909.

Chen, Z., K.A. Vallega, H. Chen, J. Zhou, S.S. Ramalingam, and S.Y. Sun. 2022. The natural product berberine synergizes with osimertinib preferentially against MET-amplified osimertinib-resistant lung cancer via direct MET inhibition. *Pharmacol. Res.* 175:105998. https://doi.org/10.1016/j.phrs.2021.105998

Chen, Z., K.A. Vallega, D. Wang, Z. Quan, S. Fan, Q. Wang, T. Leal, S.S. Ramalingam, and S.Y. Sun. 2024. DNA topoisomerase II inhibition potentiates osimertinib's therapeutic efficacy in EGFR-mutant non-small cell lung cancer models. *J. Clin. Invest.* 134:e172716. https://doi.org/10.1172/JCI172716

Chen, Z., J. Wang, Y. Bai, S. Wang, X. Yin, J. Xiang, X. Li, M. He, X. Zhang, T. Wu, et al. 2017. The associations of TERT-CLPTM1L variants and TERT mRNA expression with the prognosis of early stage non-small cell lung cancer. *Cancer Gene Ther.* 24:20–27. https://doi.org/10.1038/cgt.2016.74

Chen, Z., D. Yu, T.K. Owonikoko, S.S. Ramalingam, and S.Y. Sun. 2021. Induction of SREBP1 degradation coupled with suppression of SREBP1-mediated lipogenesis impacts the response of EGFR mutant NSCLC cells to osimertinib. *Oncogene.* 40:6653–6665. https://doi.org/10.1038/s41388-021-02057-0

Chmielecki, J., J.E. Gray, Y. Cheng, Y. Ohe, F. Imamura, B.C. Cho, M.C. Lin, M. Majem, R. Shah, Y. Rukazenkov, et al. 2023. Candidate mechanisms of acquired resistance to first-line osimertinib in EGFR-mutated advanced non-small cell lung cancer. *Nat. Commun.* 14:1070. https://doi.org/10.1038/s41467-023-35961-y

Cookson, J.C., F. Dai, V. Smith, R.A. Heald, C.A. Laughton, M.F. Stevens, and A.M. Burger. 2005. Pharmacodynamics of the G-quadruplex-stabilizing telomerase inhibitor 3,11-difluoro-6,8,13-trimethyl-8H-quino[4,3,2-kl] acridinium methosulfate (RHPS4) in vitro: Activity in human tumor cells correlates with telomere length and can be enhanced, or antagonized, with cytotoxic agents. *Mol. Pharmacol.* 68:1551–1558. https://doi.org/10.1124/mol.105.013300

Deng, Y., S.S. Chan, and S. Chang. 2008. Telomere dysfunction and tumour suppression: The senescence connection. *Nat. Rev. Cancer.* 8:450–458. https://doi.org/10.1038/nrc2393

Ding, X., J. Cheng, Q. Pang, X. Wei, X. Zhang, P. Wang, Z. Yuan, and D. Qian. 2019. BIBR1532, a selective telomerase inhibitor, enhances radiosensitivity of non-small cell lung cancer through increasing telomere dysfunction and ATM/CHK1 inhibition. *Int. J. Radiat. Oncol. Biol. Phys.* 105:861–874. https://doi.org/10.1016/j.ijrobp.2019.08.009

Dratwa, M., B. Wysoczańska, P. Łacina, T. Kubik, and K. Bogunia-Kubik. 2020. TERT-regulation and roles in cancer formation. *Front. Immunol.* 11:589929. https://doi.org/10.3389/fimmu.2020.589929

Elrod, H.A., S. Fan, S. Muller, G.Z. Chen, L. Pan, M. Tighiouart, D.M. Shin, F.R. Khuri, and S.Y. Sun. 2010. Analysis of death receptor 5 and caspase-8 expression in primary and metastatic head and neck squamous cell carcinoma and their prognostic impact. *PLoS One.* 5:e12178. https://doi.org/10.1371/journal.pone.0012178

Farré, D., R. Roset, M. Huerta, J.E. Adsuara, L. Roselló, M.M. Albà, and X. Messeguer. 2003. Identification of patterns in biological sequences at the ALGGEN server: PROMO and MALGEN. *Nucleic Acids Res.* 31:3651–3653. https://doi.org/10.1093/nar/gkg605

Ghareghomi, S., S. Ahmadian, N. Zarghami, and H. Kahroba. 2021. Fundamental insights into the interaction between telomerase/TERT and intracellular signaling pathways. *Biochimie.* 181:12–24. https://doi.org/10.1016/j.biochi.2020.11.015

Gowan, S.M., R. Heald, M.F. Stevens, and L.R. Kelland. 2001. Potent inhibition of telomerase by small-molecule pentacyclic acridines capable of interacting with G-quadruplexes. *Mol. Pharmacol.* 60:981–988. https://doi.org/10.1124/mol.60.5.981

Gu, J., W. Yang, P. Shi, G. Zhang, T.K. Owonikoko, S.R. Ramalingam, and S.Y. Sun. 2020. MEK or ERK inhibition effectively abrogates emergence of acquired osimertinib resistance in the treatment of EGFR-mutant lung cancers. *Cancer.* 126:3788–3799. https://doi.org/10.1002/cncr.32996

Guterres, A.N., and J. Villanueva. 2020. Targeting telomerase for cancer therapy. *Oncogene.* 39:5811–5824. https://doi.org/10.1038/s41388-020-01405-w

Hara, H., K. Yamashita, J. Shinada, H. Yoshimura, and T. Kameya. 2001. Clinicopathologic significance of telomerase activity and hTERT mRNA expression in non-small cell lung cancer. *Lung Cancer.* 34:219–226. https://doi.org/10.1016/S0169-5002(01)00244-6

Hayer, A., L. Shao, M. Chung, L.M. Joubert, H.W. Yang, F.C. Tsai, A. Bisaria, E. Betzig, and T. Meyer. 2016. Engulfed cadherin fingers are polarized junctional structures between collectively migrating endothelial cells. *Nat. Cell Biol.* 18:1311–1323. https://doi.org/10.1038/ncb3438

Hsu, C.P., L.W. Lee, S.C. Tang, I.L. Hsin, Y.W. Lin, and J.L. Ko. 2015. Epidermal growth factor activates telomerase activity by direct binding of Ets-2 to hTERT promoter in lung cancer cells. *Tumour Biol.* 36:5389–5398. https://doi.org/10.1007/s13277-015-3204-x

Lin, C., Y. Qin, H. Zhang, M.Y. Gao, and Y.F. Wang. 2018. EGF upregulates RFPL3 and hTERT via the MEK signaling pathway in non-small cell lung cancer cells. *Oncol. Rep.* 40:29–38. https://doi.org/10.3892/or.2018.6417

Lipinska, N., A. Romaniuk, A. Paszel-Jaworska, E. Toton, P. Kopczynski, and B. Rubis. 2017. Telomerase and drug resistance in cancer. *Cell. Mol. Life Sci.* 74:4121–4132. https://doi.org/10.1007/s00018-017-2573-2

Mender, I., S. Gryaznov, Z.G. Dikmen, W.E. Wright, and J.W. Shay. 2015. Induction of telomere dysfunction mediated by the telomerase substrate precursor 6-thio-2′-deoxyguanosine. *Cancer Discov.* 5:82–95. https://doi.org/10.1158/2159-8290.CD-14-0609

Mender, I., R. LaRanger, K. Luitel, M. Peyton, L. Girard, T.P. Lai, K. Batten, C. Cornelius, M.P. Dalvi, M. Ramirez, et al. 2018. Telomerase-Mediated strategy for overcoming non-small cell lung cancer targeted therapy and chemotherapy resistance. *Neoplasia.* 20:826–837. https://doi.org/10.1016/j.neo.2018.06.002

Mender, I., A. Zhang, Z. Ren, C. Han, Y. Deng, S. Siteni, H. Li, J. Zhu, A. Vemula, J.W. Shay, and Y.X. Fu. 2020. Telomere stress potentiates STING-dependent anti-tumor immunity. *Cancer Cell.* 38:400–411.e6. https://doi.org/10.1016/j.ccell.2020.05.020

Messeguer, X., R. Escudero, D. Farré, O. Núñez, J. Martínez, and M.M. Albà. 2002. PROMO: Detection of known transcription regulatory elements using species-tailored searches. *Bioinformatics.* 18:333–334. https://doi.org/10.1093/bioinformatics/18.2.333

Metzger, R., D. Vallbohmer, C. Müller-Tidow, H. Higashi, E. Bollschweiler, U. Warnecke-Eberz, J. Brabender, S.E. Baldus, H. Xi, W.E. Berdel, et al. 2009. Increased human telomerase reverse transcriptase (hTERT) mRNA expression but not telomerase activity is related to survival in curatively resected non-small cell lung cancer. *Anticancer Res.* 29:1157–1162.

Misawa, M., T. Tauchi, G. Sashida, A. Nakajima, K. Abe, J.H. Ohyashiki, and K. Ohyashiki. 2002. Inhibition of human telomerase enhances the effect of chemotherapeutic agents in lung cancer cells. *Int. J. Oncol.* 21:1087–1092. https://doi.org/10.3892/ijo.21.5.1087

Pfahl, M., M. Tzukerman, X.K. Zhang, J.M. Lehmann, T. Hermann, K.N. Wills, and G. Graupner. 1990. Nuclear retinoic acid receptors: Cloning, analysis, and function. *Methods Enzymol.* 189:256–270. https://doi.org/10.1016/0076-6879(90)89297-U

Piper-Vallillo, A.J., L.V. Sequist, and Z. Piotrowska. 2020. Emerging treatment paradigms for EGFR-mutant lung cancers progressing on osimertinib: A review. *J. Clin. Oncol.* 38:JCO1903123. https://doi.org/10.1200/JCO.19.03123

Ramalingam, S.S., J. Vansteenkiste, D. Planchard, B.C. Cho, J.E. Gray, Y. Ohe, C. Zhou, T. Reungwetwattana, Y. Cheng, B. Chewaskulyong, et al. 2020. Overall survival with osimertinib in untreated, EGFR-mutated advanced NSCLC. *N. Engl. J. Med.* 382:41–50. https://doi.org/10.1056/NEJMoa1913662

Seimiya, H., T. Oh-hara, T. Suzuki, I. Naasani, T. Shimazaki, K. Tsuchiya, and T. Tsuruo. 2002. Telomere shortening and growth inhibition of human cancer cells by novel synthetic telomerase inhibitors MST-312, MST-295, and MST-1991. *Mol. Cancer Ther.* 1:657–665.

Shi, P., Y.T. Oh, L. Deng, G. Zhang, G. Qian, S. Zhang, H. Ren, G. Wu, B. Legendre Jr., E. Anderson, et al. 2017. Overcoming acquired resistance to AZD9291, A third-generation EGFR inhibitor, through modulation of MEK/ERK-dependent Bim and mcl-1 degradation. *Clin. Cancer Res.* 23:6567–6579. https://doi.org/10.1158/1078-0432.CCR-17-1574

Siegel, R.L., K.D. Miller, H.E. Fuchs, and A. Jemal. 2022. Cancer statistics, 2022. *CA Cancer J. Clin.* 72:7–33. https://doi.org/10.3322/caac.21708

Suenaga, M., A. Yamaguchi, H. Soda, K. Orihara, Y. Tokito, Y. Sakaki, M. Umehara, K. Terashi, N. Kawamata, M. Oka, et al. 2006. Anti-proliferative effects of gefitinib are associated with suppression of E2F-1 expression and telomerase activity. *Anticancer Res.* 26:3387–3391.

Sun, S.Y. 2023. Taking early preventive interventions to manage the challenging issue of acquired resistance to third-generation EGFR inhibitors. *Chin. Med. J. Pulm. Crit. Care Med.* 1:3–10. https://doi.org/10.1016/j.pccm.2022.10.001

Sun, S.Y., P. Yue, M.I. Dawson, B. Shroot, S. Michel, W.W. Lamph, R.A. Heyman, M. Teng, R.A. Chandraratna, K. Shudo, et al. 1997. Differential effects of synthetic nuclear retinoid receptor-selective retinoids on the growth of human non-small cell lung carcinoma cells. *Cancer Res.* 57:4931–4939.

Van den Berg, R.M., H. Brokx, A. Vesin, J.K. Field, C. Brambilla, C.J. Meijer, G.T. Sutedja, D.A. Heideman, P.E. Postmus, E.F. Smit, and P.J. Snijders. 2010. Prognostic value of hTERT mRNA expression in surgical samples of lung cancer patients: The European early lung cancer project. *Int. J. Oncol.* 37:455–461. https://doi.org/10.3892/ijo_00000694

Veldman, T., I. Horikawa, J.C. Barrett, and R. Schlegel. 2001. Transcriptional activation of the telomerase hTERT gene by human papillomavirus type 16 E6 oncoprotein. *J. Virol.* 75:4467–4472. https://doi.org/10.1128/JVI.75.9.4467-4472.2001

Veldman, T., X. Liu, H. Yuan, and R. Schlegel. 2003. Human papillomavirus E6 and Myc proteins associate in vivo and bind to and cooperatively activate the telomerase reverse transcriptase promoter. *Proc. Natl. Acad. Sci. USA.* 100:8211–8216. https://doi.org/10.1073/pnas.1435900100

Wang, K., R.L. Wang, J.J. Liu, J. Zhou, X. Li, W.W. Hu, W.J. Jiang, and N.B. Hao. 2018. The prognostic significance of hTERT overexpression in cancers: A systematic review and meta-analysis. *Medicine.* 97:e11794. https://doi.org/10.1097/MD.0000000000011794

Wang, L., J.C. Soria, B.L. Kemp, D.D. Liu, L. Mao, and F.R. Khuri. 2002. hTERT expression is a prognostic factor of survival in patients with stage I non-small cell lung cancer. *Clin. Cancer Res.* 8:2883–2889.

Wu, T.C., P. Lin, C.P. Hsu, Y.J. Huang, C.Y. Chen, W.C. Chung, H. Lee, and J.L. Ko. 2003. Loss of telomerase activity may be a potential favorable prognostic marker in lung carcinomas. *Lung Cancer.* 41:163–169. https://doi.org/10.1016/S0169-5002(03)00195-8

Yuan, X., C. Larsson, and D. Xu. 2019. Mechanisms underlying the activation of TERT transcription and telomerase activity in human cancer: Old actors and new players. *Oncogene.* 38:6172–6183. https://doi.org/10.1038/s41388-019-0872-9

Zalaquett, Z., M. Catherine Rita Hachem, Y. Kassis, S. Hachem, R. Eid, H. Raphael Kourie, and D. Planchard. 2023. Acquired resistance mechanisms to osimertinib: The constant battle. *Cancer Treat. Rev.* 116:102557. https://doi.org/10.1016/j.ctrv.2023.102557

Zalewska-Ziob, M., K. Dobija-Kubica, K. Biernacki, B. Adamek, J. Kasperczyk, K. Bruliński, and Z. Ostrowska. 2017. Clinical and prognostic value of hTERT mRNA expression in patients with non-small-cell lung cancer. *Acta Biochim. Pol.* 64:641–646. https://doi.org/10.18388/abp.2017_1618

Zhang, S., Z. Chen, P. Shi, S. Fan, Y. He, Q. Wang, Y. Li, S.S. Ramalingam, T.K. Owonikoko, S.Y. Sun, and S.Y. Sun. 2021. Downregulation of death receptor 4 is tightly associated with positive response of EGFR mutant lung cancer to EGFR-targeted therapy and improved prognosis. *Theranostics.* 11:3964–3980. https://doi.org/10.7150/thno.54824

Zhu, C.Q., J.C. Cutz, N. Liu, D. Lau, F.A. Shepherd, J.A. Squire, and M.S. Tsao. 2006. Amplification of telomerase (hTERT) gene is a poor prognostic marker in non-small-cell lung cancer. *Br. J. Cancer.* 94:1452–1459. https://doi.org/10.1038/sj.bjc.6603110

Zhu, L., Z. Chen, H. Zang, S. Fan, J. Gu, G. Zhang, K.D. Sun, Q. Wang, Y. He, T.K. Owonikoko, et al. 2021. Targeting c-Myc to overcome acquired resistance of EGFR mutant NSCLC cells to the third-generation EGFR tyrosine kinase inhibitor, osimertinib. *Cancer Res.* 81:4822–4834. https://doi.org/10.1158/0008-5472.CAN-21-0556

Supplemental material

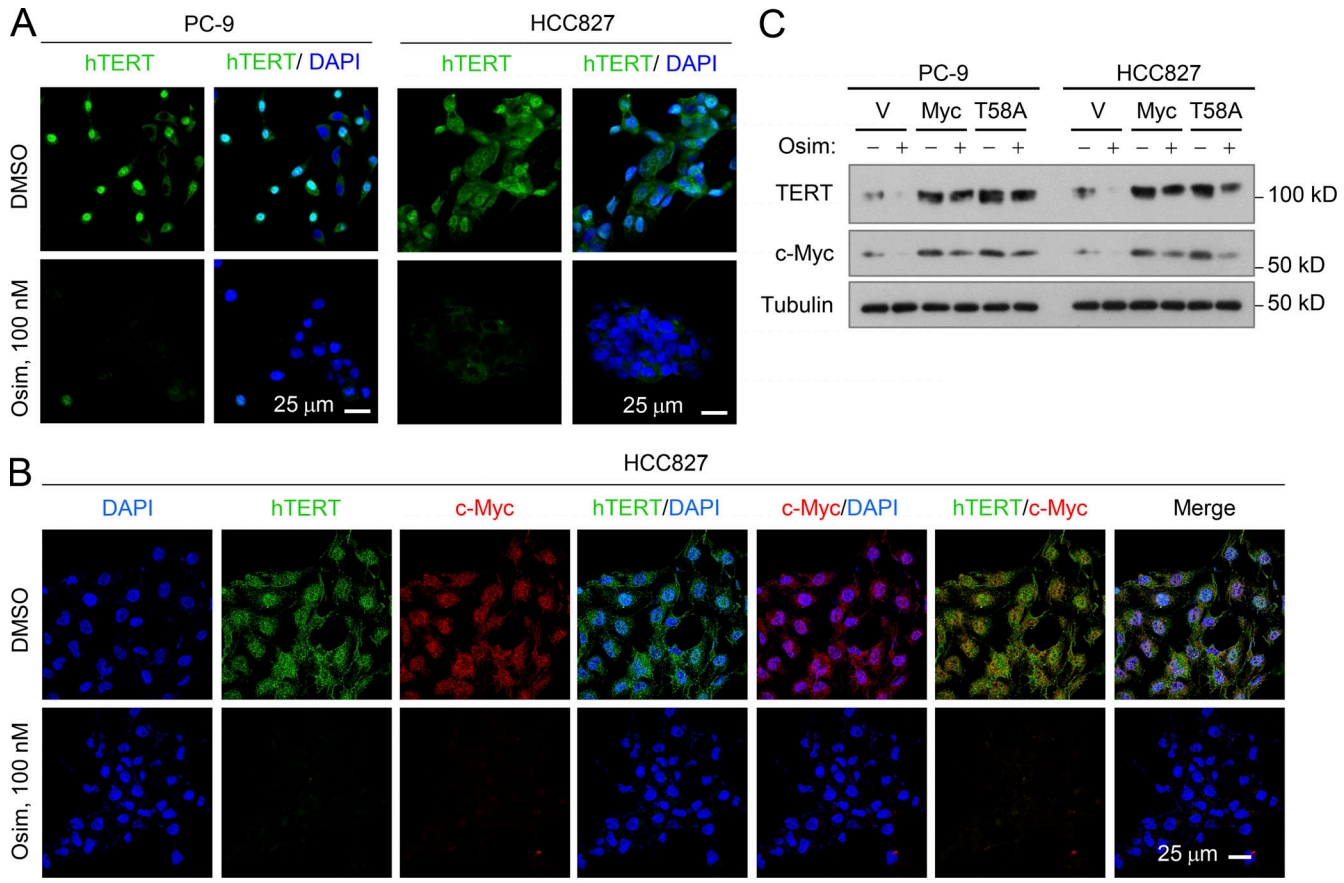

Figure S1. **c-Myc positive regulation of hTERT in EGFRm NSCLC cells. (A and B)** IF detection of hTERT (A) or hTERT and c-Myc (B). The indicated cell lines were exposed to DMSO or 100 nM osimertinib for 24 h. **(C)** Osimertinib modulation of hTERT in EGFRm NSCLC cell lines expressing ectopic c-*Myc* or c-*Myc* (T58A) gene. The treatment condition was the same for Fig. 2 G. Source data are available for this figure: SourceData FS1.

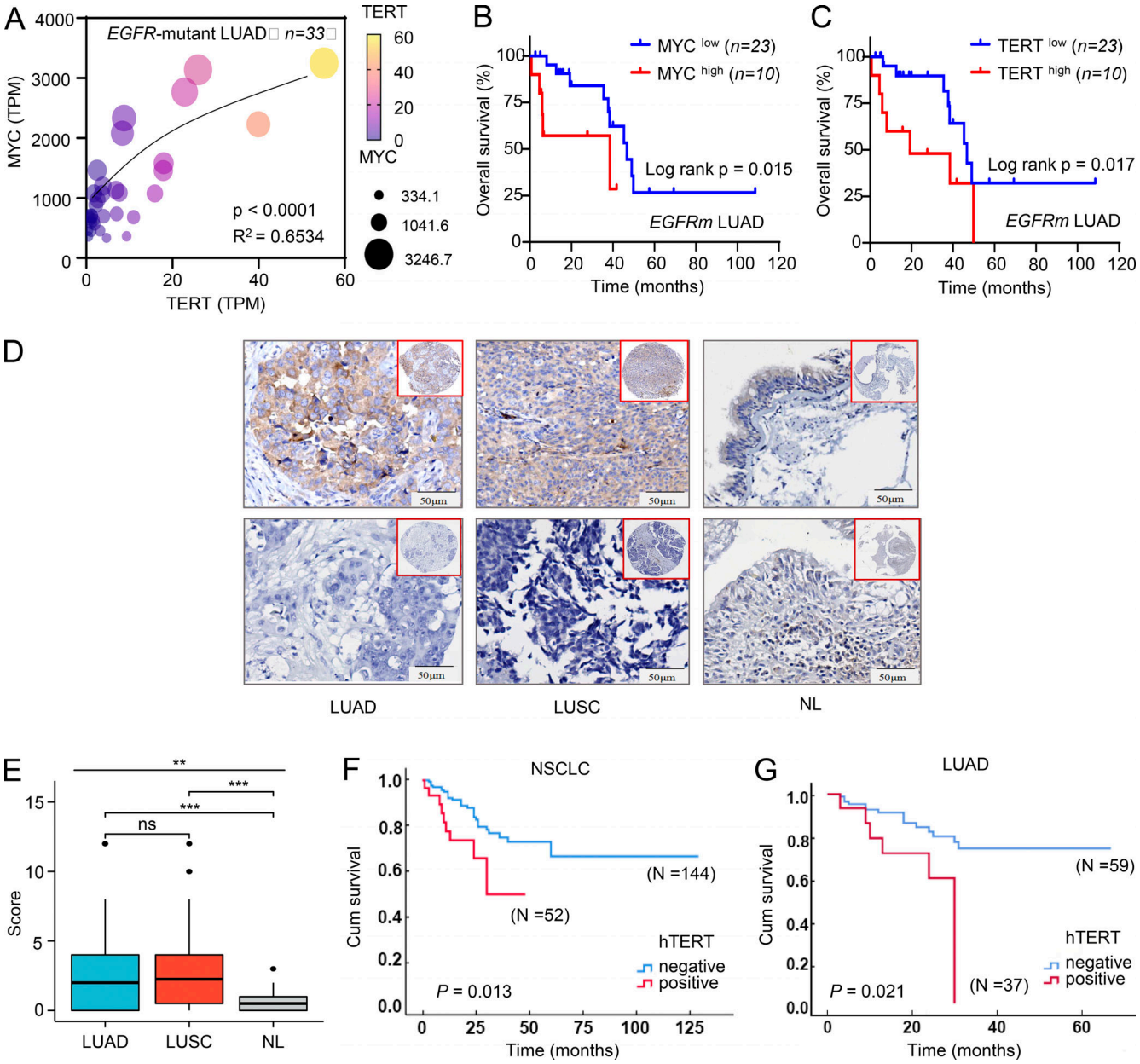

Figure S2. **hTERT expression in human NSCLC tissues, its association with c-Myc expression, and its impact on patient survival. (A–C)** TCGA data analysis of the correlation between *c-Myc* and *hTERT* expression (A) and their respective impact on patient survival (B and C) in EGFRm lung adenocarcinomas. **(A)** *c-Myc* and *hTERT* mRNA expression data from 33 EGFRm lung adenocarcinoma (LUAD) in the TCGA database were extracted and their correlation was then analyzed. TPM, transcripts per million. **(B and C)** High versus low expression (cutoff: median) of *hTERT* or *c-Myc* in these 33 tumors were also stratified and their impacts on patient survival were analyzed. **(D–G)** hTERT expression in human NSCLC tissues including lung adenocarcinoma (LUAD) and lung squamous cell carcinoma (LUSC) in comparison with normal tissue (NL) (D and E) and the impact of hTERT expression on patient survival (F and G). hTERT was stained with IHC. Statistical differences were assessed with two-sided unpaired Student's *t* test. **, P < 0.01; ***, P < 0.001; ns, not significant.

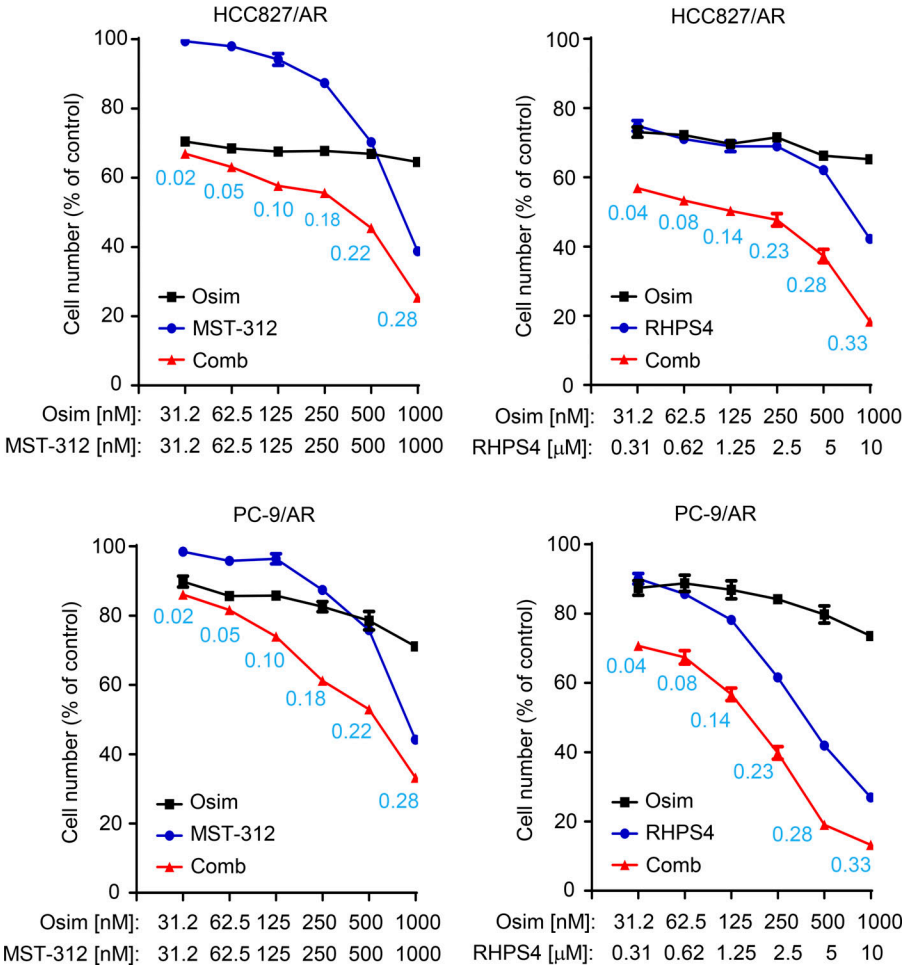

Figure S3. **Osimertinib in combination with other telomerase inhibitors synergistically decreases the survival of osimertinib-resistant cell lines.** The indicated cell lines were treated with varied concentrations of osimertinib alone, the tested telomerase inhibitor alone, or their respective combinations for 3 days. Cell numbers were determined with the SRB assay. The data are means ± SDs of four replicate determinations. The numbers in the graph by the red lines are CIs.

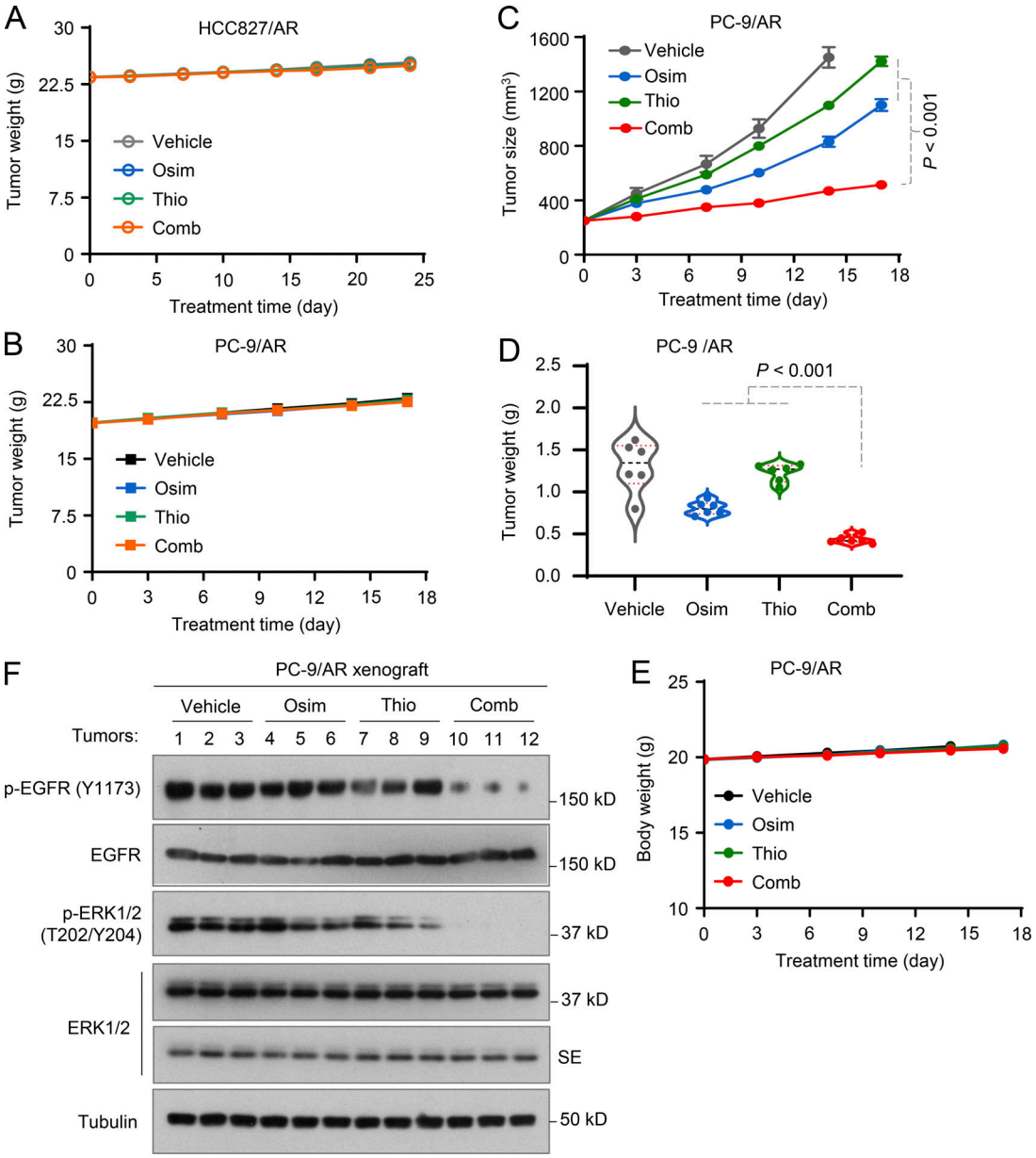

Figure S4. **Osimertinib and 6-Thio-dG combination is well tolerated in nude mice, inhibits the growth of osimertinib-resistant tumors, and suppresses EGFR/ERK signaling. (A, B, and F)** Treatments were the same as described in Fig. 6. SE, short exposure. **(C–E)** Treatments were the same as described in Fig. 6 except for the initial tumor sizes, which were over 200 mm^3, and osimertinib dosage, which was 15 mg/kg/day. Mice in the vehicle group were sacrificed a few days early before the end of the experiment. The data in each group are means ± SEs of six tumors from six mice. Statistical analysis was conducted with one-way ANOVA test. Source data are available for this figure: SourceData FS4.

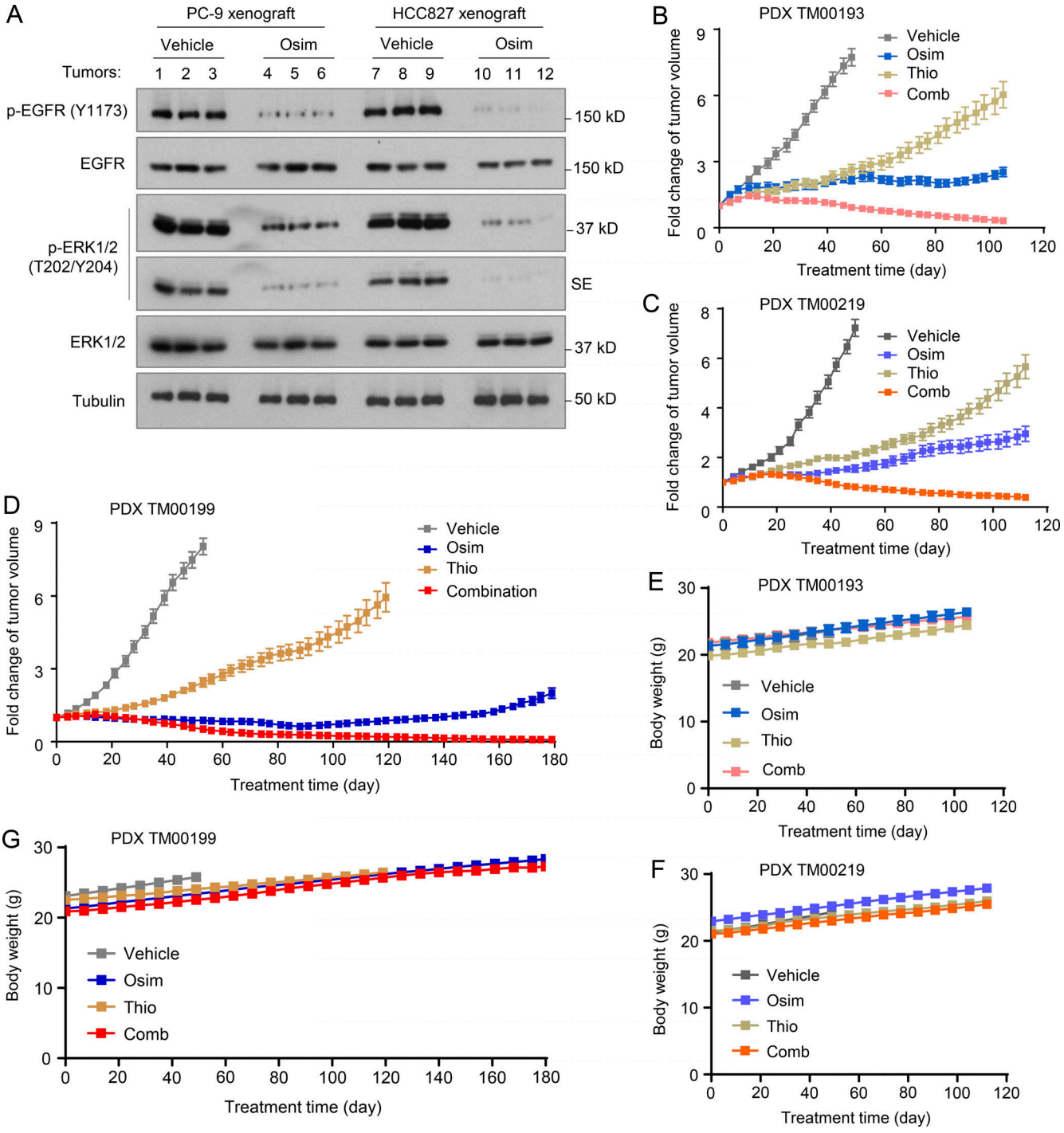

Figure S5. **Osimertinib suppresses EGFR signaling and, when combined with 6-Thio-dG, is well-tolerated in vivo. (A)** The indicated tumors at sizes of around 100 mm^3 (n = 3) were treated with osimertinib (Osim; 5 mg/kg/day, og) for 18 (PC-9) or 21 (HCC827) days. SE, short exposure. **(B–F)** Treatments were the same as described in Fig. 7. Tumor growth is presented as a fold change in tumor sizes in comparison with their initial sizes of PDXs. Source data are available for this figure: SourceData FS5.